Spectral, Structural, and Electrochemical Properties of Ruthenium Porphyrin Diaryl and Aryl(alkoxycarbonyl) Carbene Complexes: Influence of Carbene Substituents, Porphyrin Substituents, and *trans*-Axial Ligands

Yan Li,[a] Jie-Sheng Huang,*[a] Guo-Bao Xu,[b] Nianyong Zhu,[a] Zhong-Yuan Zhou,[b] Chi-Ming Che,*[a] and Kwok-Yin Wong[b]

Abstract: A wide variety of ruthenium porphyrin carbene complexes, including [Ru(tpfpp)(CR^1R^2)] (CR^1R^2 = $C(p\text{-}C_6H_4Cl)_2$ **1b**, $C(p\text{-}C_6H_4Me)_2$ **1c**, $C(p\text{-}C_6H_4OMe)_2$ **1d**, $C(CO_2Me)_2$ **1e**, $C(p\text{-}C_6H_4NO_2)CO_2Me$ **1f**, $C(p\text{-}C_6H_4OMe)CO_2Me$ **1g**, $C(CH{=}CHPh)CO_2CH_2(CH{=}CH)_2CH_3$ **1h**), [Ru(por)(CPh_2)] (por = tdcpp **2a**, 4-Br-tpp **2b**, 4-Cl-tpp **2c**, 4-F-tpp **2d**, tpp **2e**, ttp **2f**, 4-MeO-tpp **2g**, tmp **2h**, 3,4,5-MeO-tpp **2i**), [Ru(por){C(Ph)CO_2Et}] (por = tdcpp **2j**, tmp **2k**), [Ru(tpfpp)(CPh_2)(L)] (L = MeOH **3a**, EtSH **3b**, Et_2S **3c**, MeIm **3d**, $OPPh_3$ **3e**, py **3f**), and [Ru(tpfpp){C(Ph)-CO_2R}(MeOH)] (R = $CH_2CH{=}CH_2$ **4a**, Me **4b**, Et **4c**), were prepared from the reactions of [Ru(por)(CO)] with diazo compounds $N_2CR^1R^2$ in dichloromethane and, for **3** and **4**, by further treatment with reagents L. A similar reaction of [Os(tpfpp)(CO)] with N_2CPh_2 in dichloromethane followed by treatment with MeIm gave [Os(tpfpp)(CPh_2)(MeIm)] (**3d**-Os). All these complexes were characterized by ^{1}H NMR, ^{13}C NMR, and UV/Vis spectroscopy, mass spectrometry, and elemental analyses. X-ray crystal structure determinations of **1d**, **2a**,**i**, **3a**,**b**,**d**,**e**, **4a**–**c**, and **3d**-Os revealed Ru=C distances of 1.806(3)–1.876(3) Å and an Os=C distance of 1.902(3) Å. The structure of **1d** in the solid state features a unique "bridging" carbene ligand, which results in the formation of a one-dimensional coordination polymer. Cyclic voltammograms of **1a**–**c**,**g**, **2a**–**d**,**g**–**k**, **3b**–**d**, **4a**,**b**, and **3d**-Os show a reversible oxidation couple with $E_{1/2}$ values in the range of 0.06–0.65 V (vs $Cp_2Fe^{+/0}$) that is attributable to a metal-centered oxidation. The influence of carbene substituents, porphyrin substituents, and *trans*-ligands on the Ru=C bond was examined through comparison of the chemical shifts of the pyrrolic protons in the porphyrin macrocycles (^{1}H NMR) and the M=C carbon atoms (^{13}C NMR), the potentials of the metal-centered oxidation couples, and the Ru=C distances among the various ruthenium porphyrin carbene complexes. A direct comparison among iron, ruthenium, and osmium porphyrin carbene complexes is made.

Keywords: carbene ligands · electrochemistry · macrocyclic ligands · porphyrins · ruthenium

Introduction

Transition metal carbene complexes have played a leading role in the chemistry of metal–carbon multiple bonds.[1] This important class of metal complexes exhibits diverse reactivity, such as cyclopropanation of alkenes,[1b,c,f,g,j] coupling reactions with alkynes or amines/imines,[1d,g] Diels–Alder reactions,[1g] Wittig reactions,[1g] alkene metathesis,[1e,g–i] and insertions.[1c,f,g] Our interest in metal carbene complexes lies in their reactivity in carbenoid transfer reactions, and recent investigations focused on alkene cyclopropanation with iron,[2] ruthenium,[3] or osmium[4] porphyrin catalysts. We and the groups of Woo,[5] Simonneaux,[6] Berkessel,[7] and Gross[8] have found a series of iron, ruthenium, and osmium porphyrins that are active catalysts for cyclopropanation of alkenes with diazo compounds. Of particular note is the asymmetric cyclopropanation of styrenes with ethyl diazo-

[a] Y. Li, Dr. J.-S. Huang, Dr. N. Zhu, Prof. C.-M. Che
Department of Chemistry and Open Laboratory of Chemical Biology of the Institute of Molecular Technology for Drug Discovery and Synthesis
The University of Hong Kong
Pokfulam Road (Hong Kong)
Fax: (+852) 2857-1586
E-mail: cmche@hku.hk
jshuang@hku.hk

[b] Dr. G.-B. Xu, Prof. Z.-Y. Zhou, Prof. K.-Y. Wong
Department of Applied Biology and Chemical Technology and Central Laboratory of the Institute of Molecular Technology for Drug Discovery and Synthesis
The Hong Kong Polytechnic University
Hung Hom, Kowloon (Hong Kong)

[+] Correspondence on electrochemistry should be addressed to bckywong@polyu.edu.hk

DOI: 10.1002/chem.200305758

acetate catalyzed by a chiral ruthenium porphyrin,[3a,b,7] which features up to 98% *ee*, 36:1 *trans*:*cis* diastereoselectivity, and 11 000 turnovers.[3b]

We proposed that the active intermediates in the ruthenium-porphyrin-catalyzed asymmetric cyclopropanation reactions are six-coordinate ruthenium porphyrin carbene species with a strongly *trans*-labilizing ligand.[3b] However, such active intermediates have neither been isolated nor are they readily detected by spectroscopic means. On the other hand, a handful of five- and six-coordinate ruthenium porphyrin monocarbene complexes have been isolated in pure form,[3b,9–11] some of which are remarkably stable and have been structurally characterized.[3b,10,11] It is therefore of interest to find out 1) how the ruthenium–carbene bond is affected by the carbene group and the porphyrin macrocycle, and 2) the extent to which a *trans* ligand can affect the ruthenium−carbene bond.

The present work addresses these issues in considerable detail through extensive spectral, structural, and electrochemical studies on ruthenium porphyrin carbene complexes. Because of the close relationship of ruthenium with iron and osmium, this work also facilitates direct comparison of the porphyrin carbene complexes of the three metals.[12,13] The electrochemical experiments described here are, to the best of our knowledge, the first such studies on ruthenium porphyrin carbene complexes and on nonheteroatom-stabilized carbene (except vinylcarbene) complexes of metalloporphyrins.[14] Remarkably, manipulation of the substituents on the carbene groups has allowed us to observe a unique carbene bridge in a metalloporphyrin carbene complex in the solid state.

Results

Syntheses: Ruthenium porphyrin carbene complexes **1a–h**, **2a–k**, **3a–f**, and **4a–c** (see Table 1) and osmium porphyrin carbene complex [Os(tpfpp)(CPh_2)(MeIm)] (**3d**-Os) were prepared.[15] Of these carbene complexes, only **1a** has been reported elsewhere.[16]

The five-coordinate complexes [Ru(tpfpp)(CR^1R^2)] (**1b–h**), [Ru(por)(CPh_2)] (**2a–i**), and [Ru(por){C(Ph)CO_2Et}] (**2j**,**k**) were obtained by treating [Ru(por)(CO)] with the respective diazo compounds $N_2CR^1R^2$ in dichloromethane at room temperature under argon (Scheme 1). Slow addition of $N_2CR^1R^2$ by syringe was needed to minimize catalytic decomposition of the diazo compounds by the ruthenium porphyrin. The reactions proceeded markedly more slowly for sterically encumbered porphyrins (tdcpp and tmp) than for sterically unencumbered ones (e.g., tpfpp and ttp), as monitored by TLC and UV/Vis spectroscopy. In the case of sterically unencumbered porphyrins, the reactions with tpfpp complexes proceeded much more rapidly, except when the carbene ligand contains a strongly electron-withdrawing group such as NO_2 (as in **1f**). The desired carbene complexes were isolated in 45–76% yield for por = tdcpp and tmp, and in 78–92% yield for the others. This finding suggests that electron-deficient and sterically unencumbered porphyrin auxiliaries are beneficial to the isolation of ruthenium porphyrin carbene complexes.

Recrystallization of [Ru(tpfpp)(CPh_2)] (**1a**) from dichloromethane/hexane in the presence of methanol, ethanethiol, diethyl sulfide, 1-methylimidazole, triphenylphosphane oxide, or pyridine gave the six-coordinate complexes [Ru(tpfpp)(CPh_2)(L)] (**3a–f**) in 82–96% yields (Scheme 1). The six-coordinate complexes [Ru(tpfpp){C(Ph)CO_2R}(MeOH)] (**4a–c**) were isolated in 90–95% yields from the reaction of [Ru(tpfpp)(CO)] with $N_2C(Ph)CO_2R$ in dichloromethane followed by recrystallization from dichloromethane/hexane containing methanol (Scheme 1).

However, treatment of [Ru(tpfpp)(CR^1R^2)] with isocyanides did not allow isolation of the corresponding six-coordinate ruthenium porphyrin carbene complexes. For example, addition of *tert*-butyl isocyanide to a solution of **1a** in dichloromethane readily afforded [Ru(tpfpp)(C≡N*t*Bu)$_2$] (**5**), which was isolated in 85% yield. This contrasts with the inertness of the non-porphyrin ruthenium diphenylcarbene complex [Ru(tmtaa)(CPh_2)][17] towards attack by *tert*-butyl isocyanide.

The osmium complex [Os(tpfpp)(CPh_2)(MeIm)] (**3d**-Os) was prepared in 70% yield by reaction of [Os(tpfpp)(CO)] with N_2CPh_2 under similar conditions to those for its ruthenium analogue.

Spectroscopy: Complexes **1–5** and **3d**-Os were characterized by ^{1}H NMR, ^{13}C NMR, and UV/Vis spectroscopy, along

Table 1. Ruthenium complexes discussed in this paper.

	1	2	3	4
a	[Ru(tpfpp)(CPh_2)]	[Ru(tdcpp)(CPh_2)]	[Ru(tpfpp)(CPh_2)(MeOH)]	[Ru(tpfpp){C(Ph)CO_2CH_2CH=CH_2}(MeOH)]
b	[Ru(tpfpp){C(*p*-$C_6H_4Cl)_2$}]	[Ru(4-Br-tpp)(CPh_2)]	[Ru(tpfpp)(CPh_2)(EtSH)]	[Ru(tpfpp){C(Ph)CO_2Me}(MeOH)]
c	[Ru(tpfpp){C(*p*-$C_6H_4Me)_2$}]	[Ru(4-Cl-tpp)(CPh_2)]	[Ru(tpfpp)(CPh_2)(Et_2S)]	[Ru(tpfpp){C(Ph)CO_2Et}(MeOH)]
d	[Ru(tpfpp){C(*p*-$C_6H_4OMe)_2$}]	[Ru(4-F-tpp)(CPh_2)]	[Ru(tpfpp)(CPh_2)(MeIm)]	
e	[Ru(tpfpp){C($CO_2Me)_2$}]	[Ru(tpp)(CPh_2)]	[Ru(tpfpp)(CPh_2)($OPPh_3$)]	
f	[Ru(tpfpp){C(*p*-$C_6H_4NO_2$)CO_2Me}]	[Ru(ttp)(CPh_2)]	[Ru(tpfpp)(CPh_2)(py)]	
g	[Ru(tpfpp){C(*p*-C_6H_4OMe)CO_2Me}]	[Ru(4-MeO-tpp)(CPh_2)]		
h	[Ru(tpfpp){C(CH=CHPh)CO_2CH_2(CH=$CH)_2CH_3$}]	[Ru(tmp)(CPh_2)]		
i		[Ru(3,4,5-MeO-tpp)(CPh_2)]		
j		[Ru(tdcpp){C(Ph)CO_2Et}]		
k		[Ru(tmp){C(Ph)CO_2Et}]		

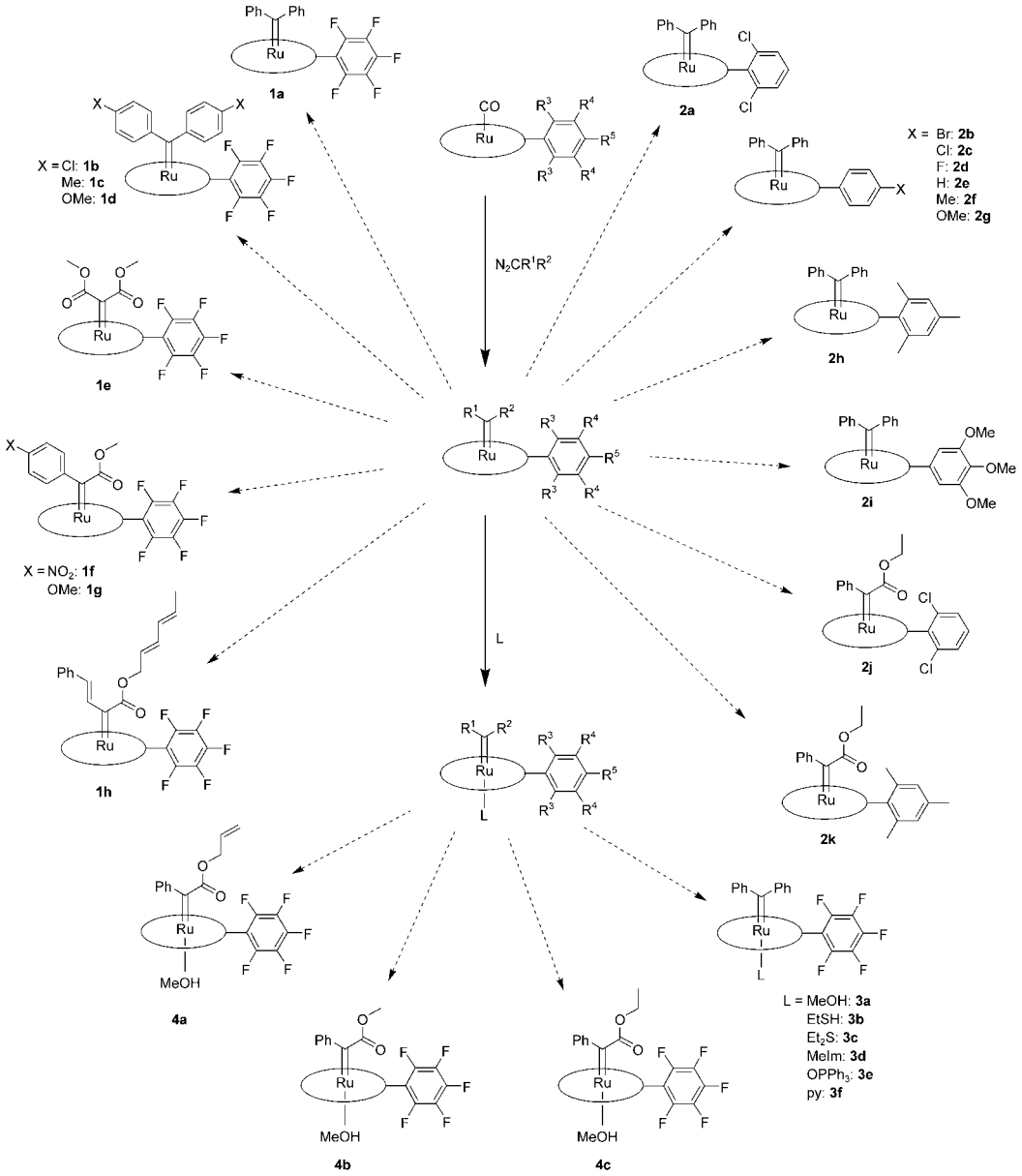

Scheme 1. Synthesis of **1a–h**, **2a–k**, **3a–f**, and **4a–c**. For clarity, only one of the four *meso*-aryl groups in each porphyrin ligand is shown.

with mass spectrometry and elemental analyses. For some of the complexes bearing the tpfpp macrocycle, ^{19}F NMR measurements were performed. A detailed compilation of the spectral data is given in the Experimental Section.

The key spectral features of **1**–**4** and **3d**-Os include: 1) sharp ^1H NMR signals at normal fields with H_β (the pyrrolic protons of the porphyrin ligands) chemical shifts of $\delta =$ 8.13–8.57 (Ru) and 7.44 (Os), 2) significantly upfield shifted ^1H NMR signals of the axial carbene groups relative to the corresponding diazo compounds [e.g., the CPh_2 signals in **2a–g** appear at $\delta \approx 6.4$ (*para*), 6.1 (*meta*), and 3.0 (*ortho*)], 3) low-field signals with $\delta = 280.49$–346.69 (Ru) and 289.27 (Os) in ^{13}C NMR spectra attributable to the $Ru{=}CR^1R^2$ or $Os{=}CR^1R^2$ carbene carbon atoms, 4) two Soret bands at about 390 and 425 nm in the UV/Vis spectra for diarylcarbene complexes of ruthenium, and a single Soret band at 388–401 (Ru) and 408 nm (Os) for the other carbene complexes of ruthenium and osmium, with the β bands appearing at 525–538 (Ru) and 519 nm (Os). These are comparable to the key spectral features of related ruthenium[3b,9,10] and osmium[4a] porphyrin carbene complexes previously reported in the literature.

For complexes [Ru(tpfpp)(CPh_2)(L)] with L = MeOH (**3a**, **4a–c**) or EtSH (**3b**), the ^1H NMR spectra do not show signals assignable to the ligands L. Probably, these complexes partially release their *trans* ligands in solution, and rapid exchange occurs between coordinated and free L on the NMR timescale, similar to the rationalization for the absence of signals for coordinated MeIm in the ^1H NMR spectrum of [Fe(tpfpp)(CPh_2)(MeIm)] (**3d**-Fe).[2] Complex **3e** with L = $OPPh_3$ has a ^1H NMR spectrum with $OPPh_3$ signals similar to those of free $OPPh_3$, that is, the *trans* $OPPh_3$ ligand dissociates from **3e** in solution.

Notably, the L signals in the ^{1}H NMR spectra of [Ru(tpfpp)(CPh$_2$)(L)] with L = Et$_2$S (**3c**), MeIm (**3d**), and py (**3f**), and **3d**-Os, are substantially upfield from those of the free ligands (see, for example, the spectra of **3c**,**d** in Figure 1). This indicates that the RuL moieties of **3c**,**d**,**f** and the Os-MeIm moiety of **3d**-Os remain intact in solution. The large upfield shifts of the signals on coordination of L to [Ru(tpfpp)(CPh$_2$)] should result mainly from the porphyrin ring-current effect.

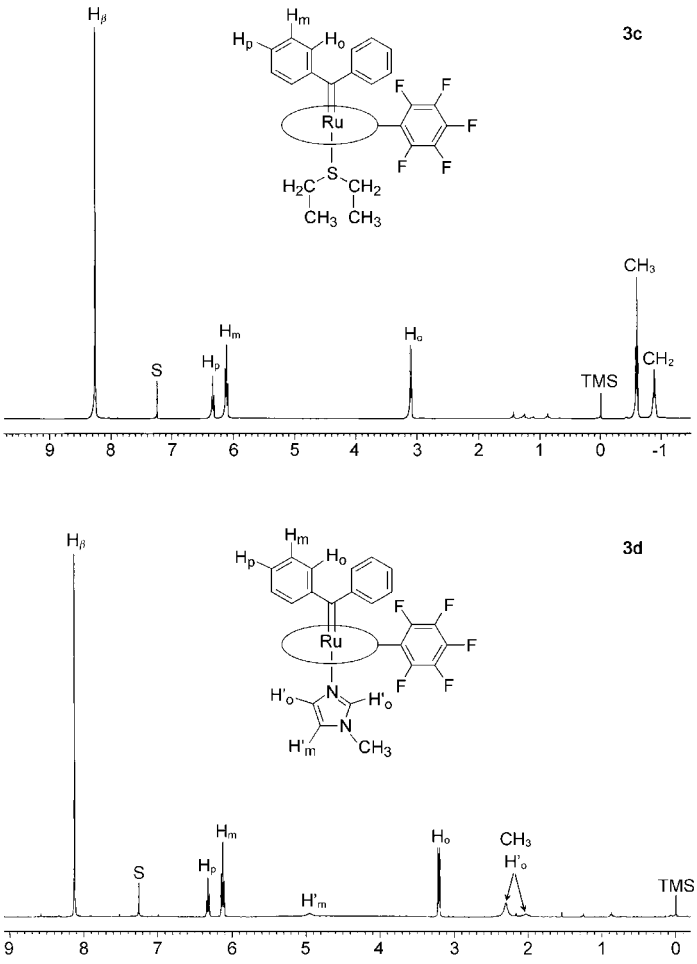

Figure 1. ^{1}H NMR spectra of **3c**,**d** in $CDCl_3$.

Bis(*tert*-butyl isocyanide)ruthenium porphyrin **5** gave H_β and *t*Bu proton signals at $\delta = 8.36$ and -0.46, respectively; its IR spectrum shows ν(C≡N) bands at 2133 and 2007 cm^{-1}. These features, along with the UV/Vis spectrum of **5** (Soret: 415 nm, β: 512 nm), are comparable to those observed for [Ru(tpp)(C≡N*t*Bu)$_2$].[18] Additionally, a low-field signal at $\delta = 182.14$ in the ^{13}C NMR spectrum of **5** can be assigned to the coordinated carbon atoms of the axial C≡N*t*Bu ligands.

X-ray crystal structures: We determined the structures of **1a**·0.5Et$_2$O, **1d**·CH$_2$Cl$_2$, **2a**·CH$_2$Cl$_2$, **2i**·CH$_2$Cl$_2$, **3a**·MeOH, **3b**,**d**,**e**, **4a**·MeOH, **4b**, **4c**·MeOH, and **3d**-Os. The structure of **1a**·0.5Et$_2$O was reported elsewhere.[16] Tables 2–4 list the crystal data and structure refinements for the other complexes; the ORTEP plots and side views of the porphyrin cores of these complexes (excluding **1d**·CH$_2$Cl$_2$) are depicted in Figures 2, 3, and 4.

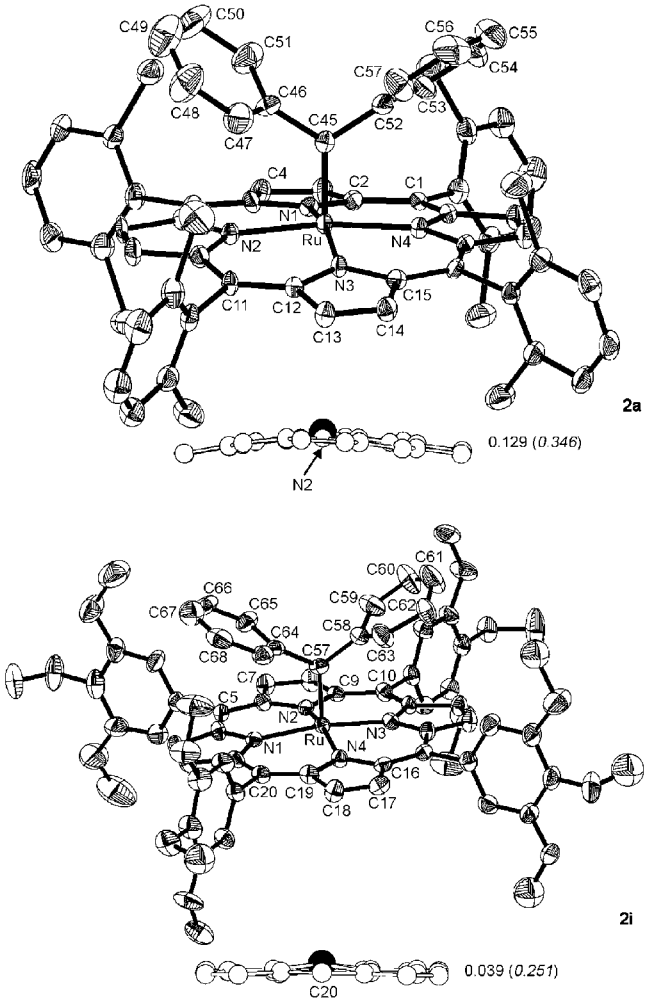

Figure 2. ORTEP plots of **2a**·CH$_2$Cl$_2$ and **2i**·CH$_2$Cl$_2$ with atom-numbering schemes (thermal ellipsoid probability: 30%). Hydrogen atoms and solvent molecules are not shown. The side views of the porphyrin rings and their mean deviations [Å] are also depicted. The displacements [Å] of Ru out of the mean porphyrin planes toward the carbene groups are given in parentheses.

The five-coordinate complexes **2a**,**i** adopt a slightly distorted square-pyramidal coordination geometry, whereas the six-coordinate complexes **3a**,**b**,**d**,**e**, **4a**–**c**, and **3d**-Os assume a distorted octahedral geometry. The porphyrin rings in both types of ruthenium/osmium porphyrin carbene complexes, except **2a**, are basically planar, with mean deviations from the least-squares planes within the range of 0.031–0.085 Å (see Figures 2–4). Complex **2a**, which bears the sterically encumbered tdcpp macrocycle, has a considerably bent porphyrin ring (see Figure 2), whose mean deviation from the least-squares plane is 0.129 Å. The ruthenium/osmium atoms lie 0.251–0.346 Å (five-coordinate complexes) and 0.134–0.193 Å (six-coordinate complexes) out of

Table 2. Crystal data and structure refinements for complexes **1d** and **2a**,**i**.

	1d·CH_2Cl_2	**2a**·CH_2Cl_2	**2i**·CH_2Cl_2
empirical formula	$C_{59}H_{22}F_{20}N_4O_2Ru{\cdot}CH_2Cl_2$	$C_{57}H_{30}Cl_8N_4Ru{\cdot}CH_2Cl_2$	$C_{69}H_{62}N_4O_{12}Ru{\cdot}CH_2Cl_2$
formula weight	1384.80	1240.45	1325.22
crystal system	monoclinic	triclinic	monoclinic
space group	$P2_1/n$	$P\bar{1}$	$C2$
a [Å]	14.611(2)	11.2455(18)	35.067(7)
b [Å]	14.604(2)	12.5185(19)	13.894(3)
c [Å]	24.801(4)	20.123(3)	16.019(3)
α [°]	90.00	85.140(4)	90
β [°]	97.329(4)	81.869(4)	113.83(3)
γ [°]	90.00	76.725(4)	90
V [Å^3]	5248.9(15)	2725.4(7)	7139(2)
Z	4	2	4
F(000)	2744	1244	2732
ρ_{calcd} [Mg m^{-3}]	1.752	1.512	1.233
$\mu(Mo_{K\alpha})$ [mm^{-1}]	0.524	0.821	0.353
index ranges	$-19 \le h \le 18$	$-11 \le h \le 14$	$-42 \le h \le 42$
	$-18 \le k \le 18$	$-10 \le k \le 16$	$-16 \le k \le 16$
	$-32 \le l \le 27$	$-26 \le l \le 26$	$-19 \le l \le 19$
reflns collected	35381	18645	19294
independent reflns	12034	12358	11801
parameters	787	658	766
final R indices ($I > 2\sigma(I)$)	$R1 = 0.054$, w$R2 = 0.11$	$R1 = 0.076$, w$R2 = 0.15$	$R1 = 0.067$, w$R2 = 0.20$
GoF	0.88	1.09	1.04
largest diff. peak/hole [e Å^{-3}]	0.928/−0.944	1.184/−0.716	1.484/−1.042

the mean porphyrin planes toward the carbene groups, as indicated in Figures 2–4.

Table 5 lists the key bond lengths and angles in **1d**, **2a**,**i**, **3a**,**b**,**d**,**e**, **4a**–**c**, and **3d**-Os, along with the corresponding bond lengths and angles in previously reported ruthenium porphyrin carbene complexes and in related iron and osmium analogues. The Ru=C distances in the new arbene complexes range from 1.806(3) to 1.876(3) Å, comparable to those in the previously reported analogues (1.829(9)–1.877(8) Å). The Os=C distance of 1.902(3) Å in **3d**-Os is similar to that in [Os(ttp)(CPh_2)(py)] (1.903(7) Å).[4b] All the metalloporphyrin carbene complexes in Table 5 have carbene angles (R^1-C-R^2) in the range of 108.0(3)–116.7(2)°, and for [M(por)(CR^1R^2)(L)] (except **3b**) the M–L distances lie in the range 2.166(4)–2.369(2) Å. The orientations of the carbene groups with respect to the porphyrin rings in these iron, ruthenium, and osmium porphyrin carbene complexes vary significantly, as reflected in the average values α of the torsion angles formed by the R^1–C and R^2–C bonds and the nearest M–N bonds, which lie in a rather wide range of about 2.4–38.9°.

Complex **3b** is a rare example of a thiol adduct of a metalloporphyrin. Collman et al. previously isolated and structurally characterized [Fe(tpp)(SPh)(PhSH)], which bears a benzenethiol group at an axial site.[19] The Ru–S distance of 2.75(1) Å in **3b** is substantially longer than those of 2.361(1)–2.377(2) Å in the thioether adducts [Ru(oep)(R^1SR^2)$_2$] (R^1SR^2 = Ph_2S, $MeSC_{10}H_{22}$)[20a] and [Ru(oep)($MeSC_{10}H_{22}$)$_2$]BF_4,[20b] and is longer than the Fe–S(PhSH) distance (2.43(2) Å) in [Fe(tpp)(SPh)(PhSH)].[19] Evidently, the ruthenium–ethanethiol interaction in **3b** is considerably weaker than the ruthenium–thioether interaction in the thioether adducts.

Table 3. Crystal data and structure refinements for complexes **3a**,**b**,**d**,**e** and **3d**-Os.

	3a·MeOH	**3b**	**3d**	**3e**	**3d**-Os
empirical formula	$C_{58}H_{22}F_{20}N_4ORu{\cdot}CH_3OH$	$C_{59}H_{24}F_{20}N_4SRu$	$C_{61}H_{24}F_{20}N_6Ru$	$C_{75}H_{32}F_{20}N_4OPRu$	$C_{61}H_{24}F_{20}N_6Os$
formula weight	1299.88	1301.95	1321.93	1517.09	1411.06
crystal system	monoclinic	monoclinic	monoclinic	monoclinic	monoclinic
space group	$P2_1$	$P2_1/c$	$P2_1/c$	$P2_1/n$	$P2_1/c$
a [Å]	13.312(2)	13.104(3)	13.194(2)	17.298(4)	13.205(3)
b [Å]	25.383(4)	25.263(5)	25.282(4)	14.579(3)	25.391(6)
c [Å]	15.877(2)	16.397(3)	16.600(3)	25.303(5)	16.664(4)
α [°]	90	90	90.00	90.00	90
β [°]	105.482(3)	105.18(3)	105.912(3)	102.52(3)	105.773(5)
γ [°]	90	90	90.00	90.00	90
V [Å^3]	5170.3(12)	5239(0)	5324.9(15)	6229(2)	5377(2)
Z	4	4	4	4	4
F(000)	2576	2584	2624	3028	2752
ρ_{calcd} [Mg m^{-3}]	1.670	1.651	1.649	1.618	1.743
$\mu(Mo_{K\alpha})$ [mm^{-1}]	0.426	0.456	0.413	0.390	2.489
index ranges	$-17 \le h \le 17$	$-15 \le h \le 15$	$-15 \le h \le 17$	$-20 \le h \le 20$	$-17 \le h \le 16$
	$-32 \le k \le 18$	$-30 \le k \le 29$	$-29 \le k \le 32$	$-17 \le k \le 17$	$-32 \le k \le 30$
	$-18 \le l \le 20$	$-19 \le l \le 19$	$-21 \le l \le 12$	$-30 \le l \le 30$	$-13 \le l \le 21$
reflns collected	35099	23517	35867	43465	35490
independent reflns	16704	8719	12196	11339	12281
parameters	1551	764	794	919	794
final R indices $R1$	0.039	0.053	0.045	0.036	0.056
($I > 2\sigma(I)$) $wR2$	0.077	0.14	0.10	0.099	0.13
GoF	1.01	0.96	1.07	0.99	0.96
largest diff. peak/hole [e Å^{-3}]	0.588/−0.667	1.132/−0.718	0.886/−0.549	0.538/−0.776	1.263/−1.193

Table 4. Crystal data and structure refinements for complexes **4a**–**c**.

	4a·MeOH	**4b**	**4c**·MeOH
empirical formula	$C_{56}H_{22}F_{20}N_4O_3Ru{\cdot}CH_3OH$	$C_{54}H_{19}F_{20}N_4O_3Ru$	$C_{55}H_{22}F_{20}N_4O_3Ru{\cdot}CH_3OH$
formula weight	1311.89	1252.80	1299.88
crystal system	monoclinic	monoclinic	monoclinic
space group	*Pc*	$P2_1/c$	*Pc*
a [Å]	12.9953(18)	16.3484(16)	12.8518(13)
b [Å]	13.7625(19)	23.914(3)	13.5190(13)
c [Å]	14.866(2)	15.8439(16)	15.136(2)
α [°]	90.00	90	90.00
β [°]	104.516(3)	116.146(4)	103.422(2)
γ [°]	90.00	90	90.00
V [Å^3]	2573.9(6)	5560.4(10)	2558.0(4)
Z	2	4	2
F(000)	1304	2476	1292
ρ_{calcd} [Mg m^{-3}]	1.693	1.497	1.688
$\mu(Mo_{K\alpha})$ [mm^{-1}]	0.431	0.394	0.433
index ranges	$-16 \le h \le 15$ $-17 \le k \le 17$ $-15 \le l \le 19$	$-11 \le h \le 21$ $-31 \le k \le 30$ $-20 \le l \le 22$	$-16 \le h \le 15$ $-16 \le k \le 17$ $-15 \le l \le 19$
reflns collected	16254	37591	16936
independent reflns	8238	12732	8318
parameters	762	732	767
final *R* indices ($I > 2\sigma(I)$)	$R1 = 0.059$, w$R2 = 0.13$	$R1 = 0.087$, w$R2 = 0.16$	$R1 = 0.040$, w$R2 = 0.10$
GoF	0.75	1.16	0.89
largest diff. peak/hole [e Å^{-3}]	0.901/−0.505	1.037/−0.925	0.976/−0.244

Table 5. Selected bond lengths [Å] and angles [°] in ruthenium porphyrin carbene complexes and in related iron and osmium analogues.

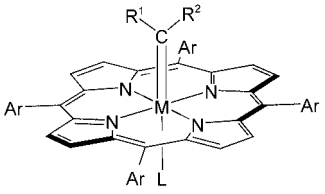

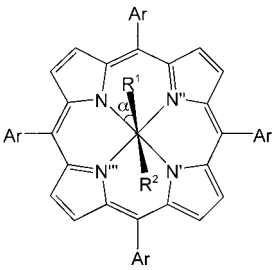

Complex	M=C	R^1-C-R^2	M−L[a]	α[b]	Ref.
[Ru(tpfpp){C(*p*-$C_6H_4OMe)_2$}] (**1d**)	1.854(4)	111.5(4)		28.5	
[Ru(tdcpp)(CPh_2)] (**2a**)	1.859(5)	110.6(4)		4.9	
[Ru(3,4,5-MeO-tpp)(CPh_2)] (**2i**)	1.866(7)	114.7(6)		2.4	
[Ru(tpfpp)(CPh_2)(MeOH)] (**3a**)	1.853(3)[c]	112.9(3)[c]	2.369(2)[c]	11.9[c]	
[Ru(tpfpp)(CPh_2)(EtSH)] (**3b**)	1.858(5)	114.2(4)	2.75(1)	8.8	
[Ru(tpfpp)(CPh_2)(MeIm)] (**3d**)	1.876(3)	113.1(2)	2.272(4)	10.8	
[Ru(tpfpp)(CPh_2)($OPPh_3$)] (**3e**)	1.853(3)	110.6(2)	2.291(3)	18.7	
[Ru(tpfpp){C(Ph)$CO_2CH_2CH{=}CH_2$}(MeOH)] (**4a**)	1.806(3)	108.0(3)	2.166(4)	15.1	
[Ru(tpfpp){C(Ph)CO_2Me}(MeOH)] (**4b**)	1.850(3)	110.6(2)	2.293(5)	6.3	
[Ru(tpfpp){C(Ph)CO_2Et}(MeOH)] (**4c**)	1.868(3)	111.6(3)	2.293(3)	18.9	
[Os(tpfpp)(CPh_2)(MeIm)] (**3d**-Os)	1.902(3)	112.8(3)	2.271(4)	9.8	
[Fe(tpfpp)(CPh_2)] (**1a**-Fe)	1.767(3)	111.5(3)		14.1	[2]
[Fe(tpfpp)(CPh_2)(MeIm)] (**3d**-Fe)	1.827(5)	111.0(4)	2.168(4)	19.2	[2]
[Ru(tpfpp)(CPh_2)] (**1a**)	1.842(4)	113.4(3)		20.6	[16]
[Ru(ttp){C(*m*-$C_6H_4CF_3)_2$}]	1.841 (6)	116.1(2)		24.3	[11c]
[Ru(por*)(CPh_2)][d]	1.860(6)	112.1(5)		38.9	[3b]
[Ru(por*){C(Ph)$CO_2CH_2CH{=}CH_2$}][d]	1.847(3)	114.3(2)		29.1	[3b]
[Ru(tpp){C(CO_2Et)$_2$}(MeOH)]	1.829(9)	112.2(7)	2.293(6)	21.4	[10]
[Ru(ttp)(CPh_2)(MeOH)]	1.845(3)	112.2(3)	2.362(3)	26.8	[11a]
[Ru(ttp){C(COPh)$_2$}(py)]	1.877(8)	116.7(2)	2.330(7)	17.4	[11b]
[Ru(ttp){C(*m*-$C_6H_4CF_3)_2$}(py)]	1.868(3)	112.8(2)	2.313(2)	32.8	[11b]
[Os(tpfpp)(CPh_2)(MeOH)] (**3a**-Os)	1.870(2)	112.3(2)	2.347(2)	11.3	[4a]

[a] M−O for L = MeOH and $OPPh_3$; M−S for L = EtSH; M−N for L = MeIm and py. [b] Average value of the R^1-C-M-N and R^2-C-M-N′ torsion angles. [c] Average value of the two independent molecules in the unit cell. [d] (por*)$^{2-}$ = 5,10,15,20-tetrakis[(1*S*,4*R*,5*R*,8*S*)-1,2,3,4,5,6,7,8-octahydro-1,4:5,8-dimethanoanthracen-9-yl]porphyrinato dianion.

The structures of **3a**·MeOH, **4a**·MeOH, and **4c**·MeOH feature hydrogen bonds between the oxygen atoms of the coordinated and uncoordinated methanol molecules, with O···O distances of about 2.67–2.89 (**3a**·MeOH), 2.78 (**4a**·MeOH), and 2.79 Å (**4c**·MeOH). The hydrogen bonding in **3a**·MeOH leads to the formation of a "methanol tetramer" lying between two [Ru(tpfpp)(CPh_2)] moieties, as depicted in Figure 5. In this regard, the structure of **3a**·MeOH in the solid state can be described as a $(MeOH)_4$-bridged metalloporphyrin dimer. Complex **4b** features hydrogen bonds between the oxygen atoms of the coordinated methanol and the carbonyl group of the carbene ligand in an adjacent molecule (O···O ca. 2.78 Å), which result in the formation of a one-dimensional polymer linked by hydrogen bonds (Figure 5).

In the solid state, complex **1d** is a one-dimensional coordination polymer,[21] as can be seen in the packing diagram shown in Figure 6. Here the bis(*p*-methoxyphenyl)carbene groups function as a unique type of bridge: each of them links two ruthenium atoms through the carbene carbon atom and one of the two methoxy oxygen atoms. Such a bridging carbene group has not been seen in any previously reported structurally characterized metalloporphyrin carbene complexes.[1j] The Ru−O distance in **1d** of 2.498(3) Å is considerably longer than those in the ruthenium porphyrin carbene complexes with MeOH or $OPPh_3$ *trans* ligands (see Table 5). The C-Ru-O moiety is basically linear and has an angle of 175.0(2)°.

One-dimensional coordination polymers of metalloporphyrins linked by carbene groups are unprecedented, although many metalloporphyrin coordination polymers linked by other ligands (e.g., imidazo-

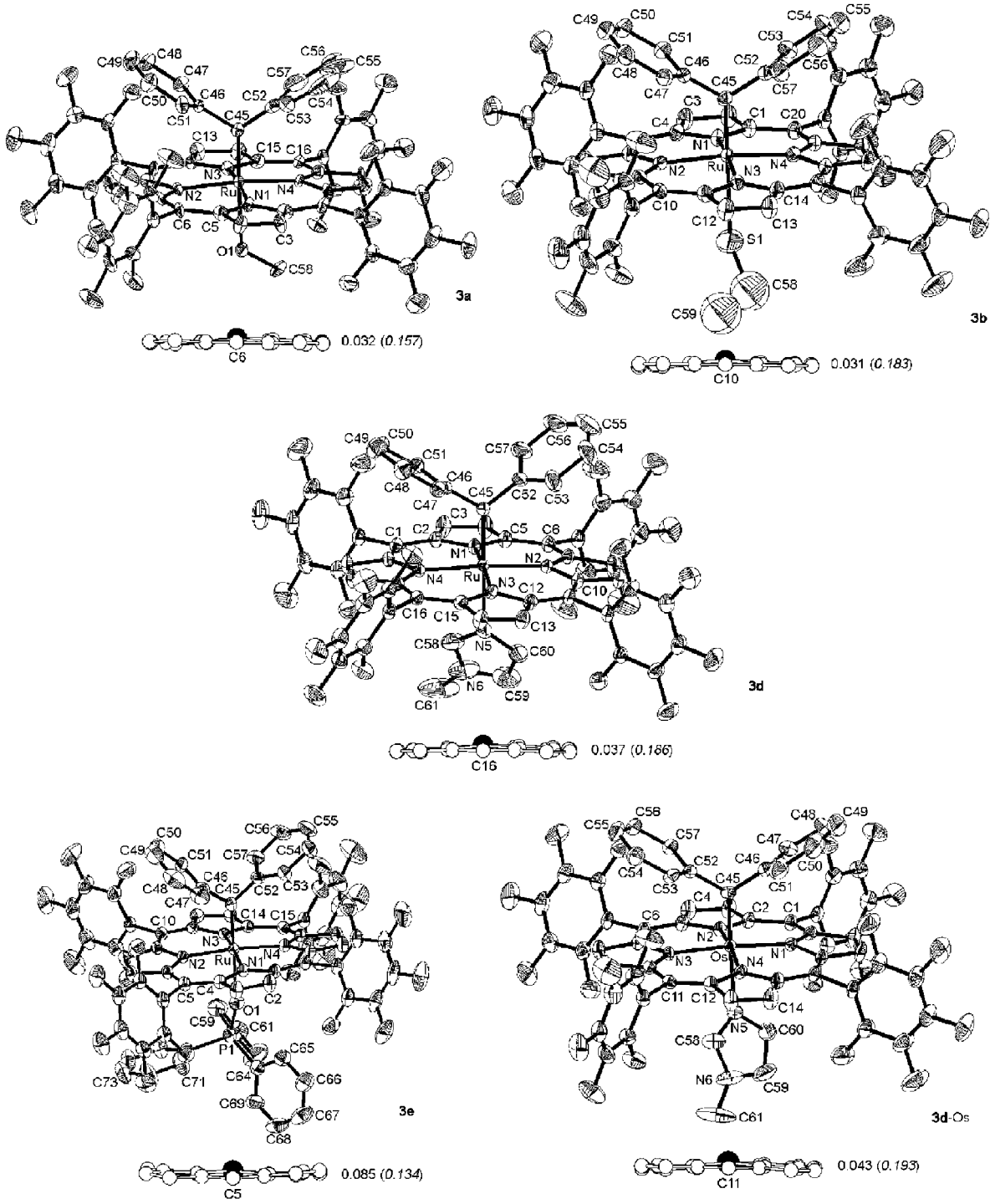

Figure 3. ORTEP plots of **3a**·MeOH (molecule a), **3b**,**d**,**e**, and **3d**-Os with atom-numbering schemes (thermal ellipsoid probability: 30%). Hydrogen atoms and solvent molecules, if any, are not shown. The side views of the porphyrin rings and their mean deviations [Å] are also depicted. The displacements [Å] of Ru or Os out of the mean porphyrin planes toward the carbene groups are given in parentheses.

late, pyrazine, and 4,4′-bipyridine) have been reported.[22] Moreover, previous examples of structurally characterized one-dimensional metalloporphyrin coordination polymers span the metal ions of Mn,[22a,b,g–j], Fe[22c], Cu,[22e] and Zn.[22f] Complex **1d** is a rare example of structurally characterized one-dimensional metalloporphyrin coordination polymer of a second-row transition metal.

Electrochemistry: Cyclic voltammetry was used to examine the redox behavior of complexes **1a–c**,**f**,**g**, **2a–d**,**g–k**, **3b–d**, **4a**,**b**, **1a**-Fe, **3d**-Fe, **3d**-Os, **5**, and [Ru(tpfpp)(CO)] in dichloromethane. The observed redox potentials (vs $Cp_2Fe^{+/0}$) for these complexes are listed in Table 6. Figure 7 shows the cyclic voltammograms of **2b**,**g**, **3d**, and **3d**-Os. To our knowledge, this is the first systematic electrochemical studies on ruthenium/osmium porphyrin carbene complexes.

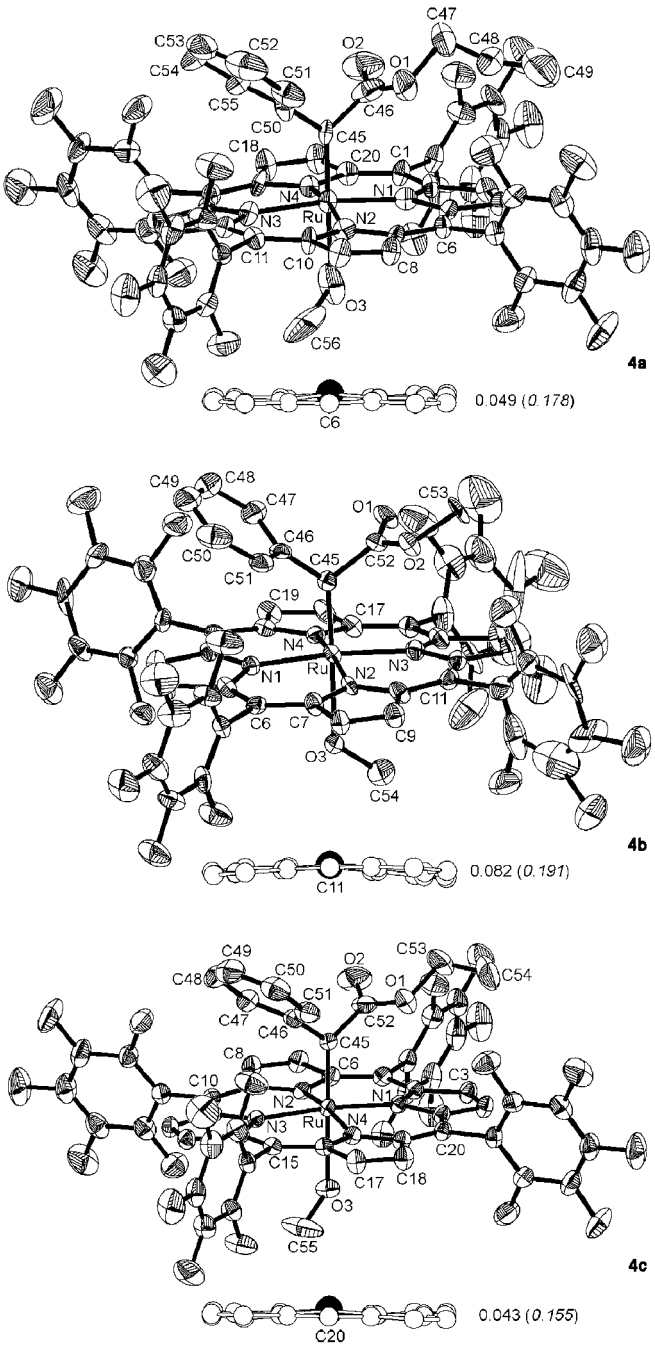

Figure 4. ORTEP plots of **4a**·MeOH, **4b**, and **4c**·MeOH with atom-numbering schemes (thermal ellipsoid probability: 30%). Hydrogen atoms and solvent molecules, if any, are not shown. The side views of the porphyrin rings and their mean deviations [Å] are also depicted. The displacements [Å] of Ru out of the mean porphyrin planes toward the carbene groups are given in parenthesis.

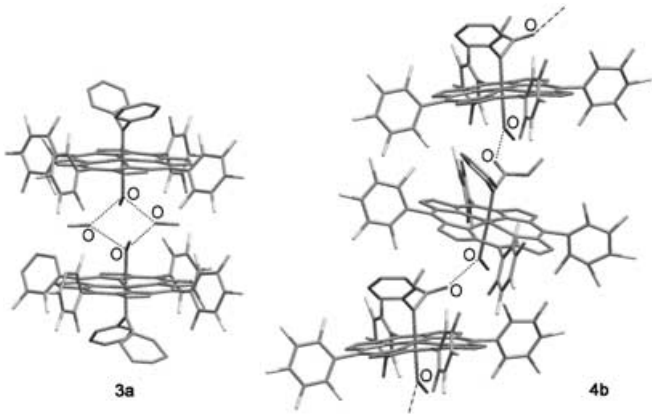

Figure 5. Hydrogen bonds in the structures of **3a**·MeOH and **4b** (the hydrogen atoms are not shown).

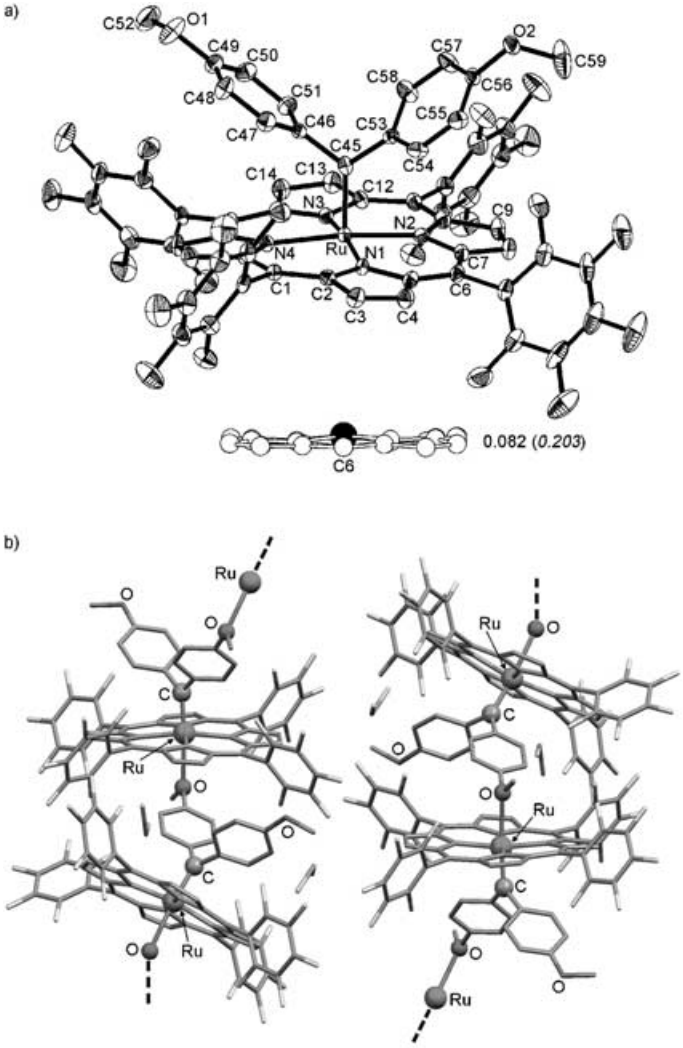

Figure 6. a) ORTEP plot of the [Ru(tpfpp){C(*p*-$C_6H_4OMe)_2$}] moiety of **1d**·CH_2Cl_2 with atom-numbering scheme (thermal ellipsoid probability level: 30%). Hydrogen atoms and the solvent molecule are not shown. The side view of the porphyrin ring, together with its mean deviation [Å], is also depicted. The displacement [Å] of Ru out of the mean porphyrin plane toward the carbene group is given in parenthesis. b) Packing diagram of **1d**·CH_2Cl_2 with omission of hydrogen atoms and cell axes.

Electrochemical studies on the other types of ruthenium/osmium porphyrins, such as carbonyl- and bis(pyridine)ruthenium/osmium porphyrins, have been reported previously.[23]

Of the metalloporphyrins listed in Table 6, the complexes bearing tpfpp and tdcpp macrocycles, except **3d**-Os, generally show one reversible oxidation couple with $E_{1/2}$ = 0.13–0.84 V. For **3d**-Os and the complexes bearing other porphyrin macrocycles (except **2g**), two reversible oxidation couples

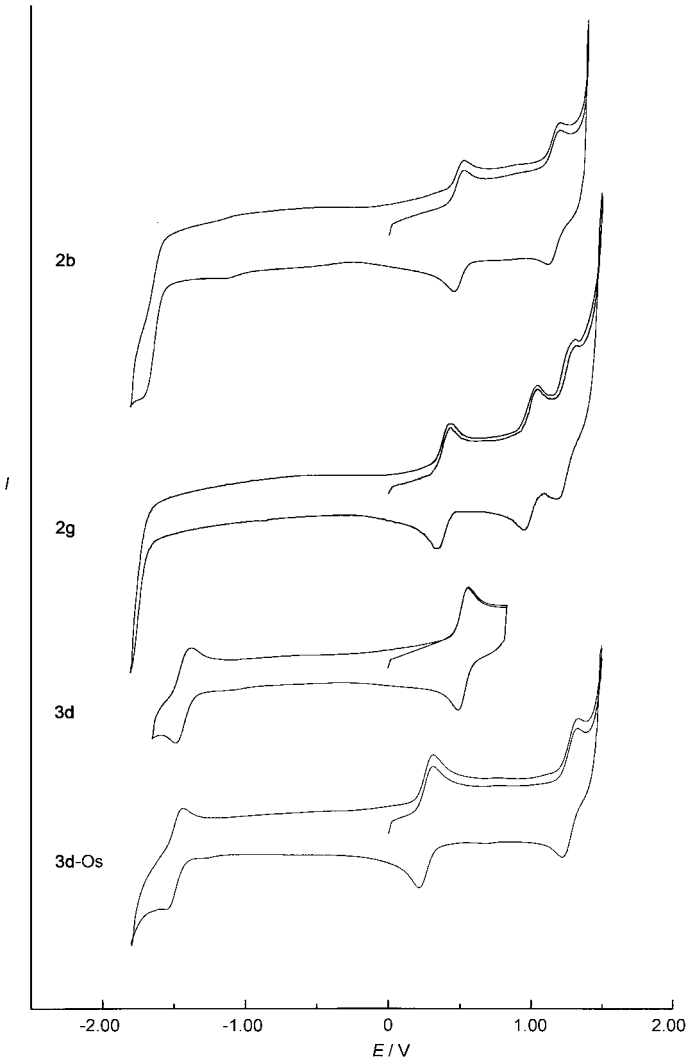

Figure 7. Cyclic voltammograms of **2b**,**g**, **3d**, and **3d**-Os in dichloromethane [V vs 0.1 M $Ag/AgNO_3$ in CH_3CN] at a scan rate of 100 mV s^{-1}.

with $E_{1/2}$ of 0.06–0.32 and 0.81–1.07 V were observed. Complex **2g** shows three reversible oxidation couples with $E_{1/2}$ = 0.20, 0.80, and 1.03 V. A reversible reduction couple with $E_{1/2}$ in the range of −1.25 to −1.73 V appears in almost all the cyclic voltammograms of the tpfpp complexes. The reduction waves of the carbene complexes bearing the other porphyrin macrocycles were probably obscured by the reduction of the solvent and in some cases were partially observable.

To help identify the oxidation couples of ruthenium porphyrin carbene complexes, we examined the spectroelectrochemistry of **2d**,**h**,**j**,**k** in dichloromethane with electrode potentials of 0.74, 0.62, 0.77, and 0.65 V, respectively. The resulting time-resolved UV/Vis spectra of **2h**,**k** are shown in Figure 8. Upon electrolysis at the above potentials, the two Soret bands of the diphenylcarbene complexes **2d**,**h** at about 395 and 430 nm collapsed into a single band, and the single Soret bands of the phenyl(ethoxycarbonyl)carbene complexes **2j**,**k** at about 398 nm underwent an appreciable red shift. The final spectra for both the diphenylcarbene and phenyl(ethoxycarbonyl)carbene complexes show a Soret

Table 6. Half-wave potentials [V vs $Cp_2Fe^{+/0}$] of iron, ruthenium, and osmium porphyrin carbene complexes (scan rate: 100 mV s^{-1}).

Complex	E_{O1}	E_{O2}	E_{R1}
[Ru(tpfpp)(CO)]	0.84		−1.61
[Fe(tpfpp)(CPh_2)] (**1a**-Fe)	0.35		−1.52
[Ru(tpfpp)(CPh_2)] (**1a**)	0.46		−1.53
[Ru(tpfpp){C(*p*-$C_6H_4Cl)_2$}] (**1b**)	0.57		−1.50
[Ru(tpfpp){C(*p*-$C_6H_4Me)_2$}] (**1c**)	0.44		−1.55
[Ru(tpfpp){C(*p*-$C_6H_4NO_2$)CO_2Me}] (**1f**)	0.77		−1.25
[Ru(tpfpp){C(*p*-C_6H_4OMe)CO_2Me}] (**1g**)	0.50		−1.51
[Ru(tdcpp)(CPh_2)] (**2a**)	0.32		−1.88[a]
[Ru(4-Br-tpp)(CPh_2)] (**2b**)	0.30	0.96	−1.89[a]
[Ru(4-Cl-tpp)(CPh_2)] (**2c**)	0.32	0.96	−1.88[a]
[Ru(4-F-tpp)(CPh_2)] (**2d**)	0.26	0.94	
[Ru(4-MeO-tpp)(CPh_2)] (**2g**)[b]	0.20	0.80	
[Ru(tmp)(CPh_2)] (**2h**)	0.19	0.98	
[Ru(3,4,5-MeO-tpp)(CPh_2)] (**2i**)	0.25	0.81	
[Ru(tdcpp){C(Ph)CO_2Et}] (**2j**)	0.42		−1.73
[Ru(tmp){C(Ph)CO_2Et}] (**2k**)	0.32	0.92	
[Ru(tpfpp)(CPh_2)(EtSH)] (**3b**)	0.52		−1.53
[Ru(tpfpp)(CPh_2)(Et_2S)] (**3c**)	0.52		−1.53
[Fe(tpfpp)(CPh_2)(MeIm)] (**3d**-Fe)	0.13		−1.67
[Ru(tpfpp)(CPh_2)(MeIm)] (**3d**)	0.33		−1.63
[Os(tpfpp)(CPh_2)(MeIm)] (**3d**-Os)	0.06	1.07	−1.71
[Ru(tpfpp){C(Ph)$CO_2CH_2CH{=}CH_2$}(MeOH)] (**4a**)	0.63		−1.46
[Ru(tpfpp){C(Ph)CO_2Me}(MeOH)] (**4b**)	0.65		−1.47
[Ru(tpfpp)(C≡N*t*Bu)$_2$] (**5**)	0.42		−1.90[a]

[a] $E_{p,c}$. [b] E_{O3} = 1.03 V.

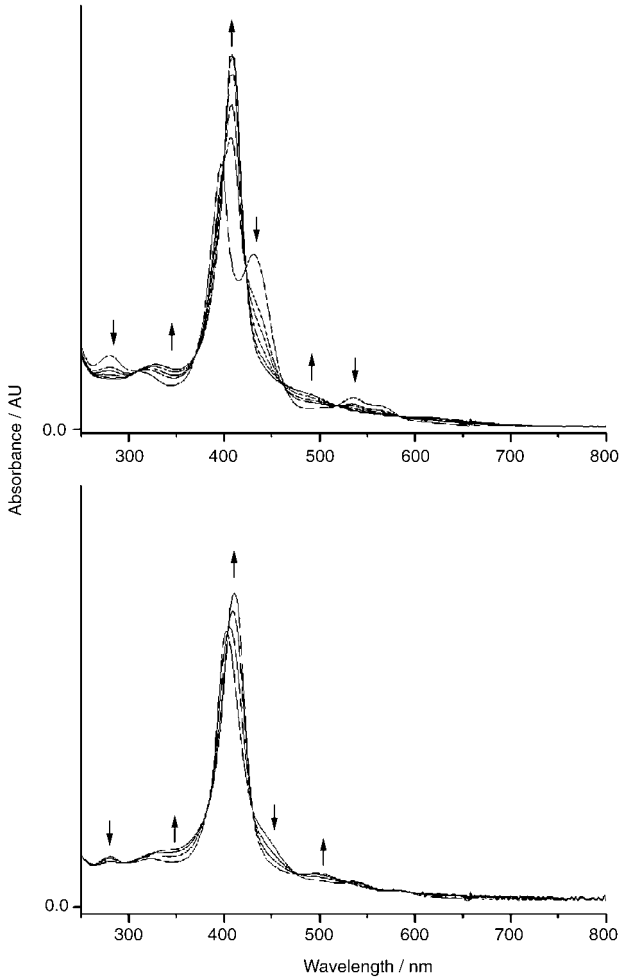

Figure 8. Spectroelectrochemistry of **2h** (top) and **2k** (bottom) in dichloromethane. Electrode potentials: 0.62 (**2h**) and 0.65 V (**2k**) vs $Cp_2Fe^{+/0}$.

band at about 410 nm, that is, the electronic spectra of the oxidized ruthenium porphyrin carbene species are less strongly affected by the carbene substituents. During the electrolysis of **2d**,**h**,**j**,**k**, no prominent bands appeared at 600–800 nm in the time-resolved UV/Vis spectra. This reveals that the corresponding oxidation processes are metal-centered, and the porphyrin rings remain unoxidized.[24]

Discussion

Ruthenium porphyrin carbene complexes have been known for about 20 years since the pioneering work by Collman et al.[9a] The porphyrin macrocycles so far employed for preparing this family of ruthenium porphyrins include tpp,[10] ttp,[9a,b,11] tmp,[9c] and por*,[3b] with the carbene ligands CHR (R = Et, $SiMe_3$, CO_2Et),[9a,b] $C(Ph)CO_2CH_2CH{=}CH_2$,[3b] and CR_2 (R = Ph,[3b,11a] *m*-$C_6H_4CF_3$,[11b,c] COPh,[11b] CO_2Et[10]). In the literature there has been no systematic examination of the influence of carbene substituents, porphyrin substituents, and *trans* ligands on the ruthenium–carbene bond.

The ruthenium carbene complexes prepared here contain a wider variety of porphyrin macrocycles, ranging from tpp, 4-Br-tpp, 4-Cl-tpp, 4-F-tpp, ttp, 4-MeO-tpp, 3,4,5-MeO-tpp to electron-deficient tpfpp, and to sterically encumbered tdcpp and tmp. The carbene groups in these new ruthenium porphyrin carbene complexes span $C(p\text{-}C_6H_4X)_2$ (X = Cl, H, Me, OMe), $C(CO_2Me)_2$, $C(p\text{-}C_6H_4X)CO_2Me$ (X = NO_2, H, OMe), $C(Ph)CO_2R$ (R = Et, $CH_2CH{=}CH_2$), and $C(CH{=}CHPh)CO_2CH_2(CH{=}CH)_2CH_3$.

Complexes **1a–h** and **4a–c** have the same [Ru(tpfpp)] and [Ru(tpfpp)(MeOH)] moiety, respectively, but contain different carbene groups, and can be employed for examination of the influence of carbene substituents by direct comparison. Direct comparisons are also possible among **1a**, **2a–i** or between **2j**,**k**; these complexes have the same $Ru{=}CPh_2$ or $Ru{=}C(Ph)CO_2Et$ moiety in common but bear different porphyrin macrocycles and are suitable for inspecting the influence of porphyrin substituents. Concerning the influence of *trans* ligands, we make direct comparisons between [Ru(tpfpp)(CPh_2)] (**1a**) and its adducts [Ru(tpfpp)(CPh_2)(L)] (**3**) and among **3a–f**. Complexes **3d**, **3d**-Os, and the previously reported iron analogue **3d**-Fe[2] would allow a comparison among the porphyrin carbene complexes of the iron subgroup.

Variation of H_β and M=C chemical shifts: It is well documented that the H_β chemical shift in the ^1H NMR spectrum of a diamagnetic metalloporphyrin increases with increasing oxidation state of the metal ion.[25] Comparison of such chemical shifts among the above metalloporphyrin carbene complexes should reveal the difference in electron density of the metal ions in these complexes and provide useful information on the electronic properties of the M=C bonds. Furthermore, the electronic properties of M=C bonds should also be correlated with the ^{13}C chemical shifts of the M=C carbon atoms. Table 7 lists the H_β and M=C chemical shifts of ruthenium porphyrin carbene complexes, together with some comparisons among carbene complexes of iron, ruthenium, and osmium porphyrins.

Table 7. Comparison of H_β and M=*C* chemical shifts (δ/ppm) among ruthenium porphyrin carbene complexes and related iron and osmium analogues.

Complex	M	por	CR^1R^2	L	H_β	M=*C*
1a	Ru	tpfpp	CPh_2		8.32	328.70
1b	Ru	tpfpp	$C(p\text{-}C_6H_4Cl)_2$		8.37	322.65
1c	Ru	tpfpp	$C(p\text{-}C_6H_4Me)_2$		8.29	333.00
1d	Ru	tpfpp	$C(p\text{-}C_6H_4OMe)_2$		8.27	324.76
1e	Ru	tpfpp	$C(CO_2Me)_2$		8.57	280.49
1f	Ru	tpfpp	$C(p\text{-}C_6H_4NO_2)CO_2Me$		8.51	299.44
1g	Ru	tpfpp	$C(p\text{-}C_6H_4OMe)CO_2Me$		8.44	298.85
1h	Ru	tpfpp	$C(CH{=}CHPh)CO_2CH_2(CH{=}CH)_2CH_3$		8.45	288.71
4a	Ru	tpfpp	$C(Ph)CO_2CH_2CH{=}CH_2$	MeOH	8.53	304.34
4b	Ru	tpfpp	$C(Ph)CO_2Me$	MeOH	8.46	304.13
4c	Ru	tpfpp	$C(Ph)CO_2Et$	MeOH	8.46	305.52
2a	Ru	tdcpp	CPh_2		8.17	327.86
2b	Ru	4-Br-tpp	CPh_2		8.33	319.70
2c	Ru	4-Cl-tpp	CPh_2		8.33	319.50
2d	Ru	4-F-tpp	CPh_2		8.32	318.70
2e	Ru	tpp	CPh_2		8.34	317.50
2f	Ru	ttp	CPh_2		8.36	316.40
2g	Ru	4-MeO-tpp	CPh_2		8.37	319.40
2h	Ru	tmp	CPh_2		8.13	318.08
2i	Ru	3,4,5-MeO-tpp	CPh_2		8.45	316.30
2j	Ru	tdcpp	$C(Ph)CO_2Et$		8.27	298.50
2k	Ru	tmp	$C(Ph)CO_2Et$		8.23	287.50
3a	Ru	tpfpp	CPh_2	MeOH	8.24	329.00
3b	Ru	tpfpp	CPh_2	EtSH	8.29	330.85
3c	Ru	tpfpp	CPh_2	Et_2S	8.26	338.34
3d	Ru	tpfpp	CPh_2	MeIm	8.13	332.13
3e	Ru	tpfpp	CPh_2	$OPPh_3$	8.30	330.15
3f	Ru	tpfpp	CPh_2	py	8.18	346.69
1a-Fe[a]	Fe	tpfpp	CPh_2		8.31	358.98
3d-Fe[a]	Fe	tpfpp	CPh_2	MeIm	8.23	385.44
3a-Os[b]	Os	tpfpp	CPh_2	MeOH	7.73	273.60
3d-Os	Os	tpfpp	CPh_2	MeIm	7.44	289.27

[a] From ref. [2]. [b] From ref. [4a].

As shown in Table 7, complexes [Ru(tpfpp)(CR^1R^2)] (**1a–h**) give gradually decreasing H_β chemical shifts along the CR^1R^2 series of $C(CO_2Me)_2 > C(p\text{-}C_6H_4NO_2)CO_2Me > C(CH{=}CHPh)CO_2CH_2(CH{=}CH)_2CH_3$, $C(p\text{-}C_6H_4OMe)CO_2Me > C(p\text{-}C_6H_4Cl)_2 > CPh_2 > C(p\text{-}C_6H_4Me)_2$, $C(p\text{-}C_6H_4OMe)_2$. This is consistent with the increase in electron-donating capability, or decrease in electron-withdrawing ca-

pability, of the carbene group along the above sequence. Indeed, a more strongly electron-donating carbene group would increase the electron density of the ruthenium ion and thus correspond to a smaller H_β chemical shift.

However, in most cases the M=*C* chemical shifts of the [Ru(tpfpp)(CR^1R^2)] complexes increase with increasing electron-donating capability of the carbene group, apparently opposite to the trend due to the inductive effect. We attribute this phenomenon to competition between the inductive effect and the effect of the aryl ring current in the carbene groups. For example, although the phenyl groups in CPh_2 are more strongly electron-donating than the ester groups in $C(CO_2Me)_2$, the phenyl ring-current effect in the former deshields the carbene carbon atom to a much greater extent than the shielding from the stronger electron donors.

The similar H_β and M=*C* chemical shifts of the complexes [Ru(tpfpp){C(Ph)CO_2R}(MeOH)] (**4a–c**; R = CH_2CH=CH_2, Me, Et) reflect the fact that these carbene groups affect the electron density of the ruthenium ion to a comparable extent.

For [Ru(por)(CPh_2)] (**1a**, **2a–i**) and [Ru(por){C(Ph)-CO_2Et}] (**2j**,**k**), the Ru=*C* chemical shifts gradually decrease along the porphyrin sequence of tpfpp > tdcpp > 4-Br-tpp, 4-Cl-tpp, 4-MeO-tpp > 4-F-tpp > tmp > tpp > ttp, 3,4,5-MeO-tpp. This trend is in accord with the electron-withdrawing or -donating capability of the porphyrin macrocycles, except for the somewhat abnormal positions of 4-MeO-tpp and tmp. The dependence of the H_β chemical shifts of [Ru-(por)(CPh_2)] on the porphyrin ligand is less regular; in some cases, such as tpfpp→tdcpp, tpp→tmp, and tdcpp→tmp, the H_β chemical shift does decrease as the porphyrin ligand becomes more strongly electron-donating. Note that the differences in both H_β and M=*C* chemical shifts among 4-Br-tpp, 4-Cl-tpp, 4-MeO-tpp, 4-F-tpp, tpp, and ttp are small, and this indicates that the *para* substituents on the *meso*-phenyl groups of tpp only slightly alter the electron density of the ruthenium ion.

Complexes [Ru(tpfpp)(CPh_2)(L)] (**3**, L = EtSH, Et_2S, MeOH, py, MeIm) generally exhibit smaller H_β chemical shifts than [Ru(tpfpp)(CPh_2)] (**1a**), consistent with an increase in electron density of the ruthenium ion through electron donation from the *trans* ligands. The H_β chemical shifts of **3** follow the order of EtSH, Et_2S, MeOH > py > MeIm, which suggests that MeIm has the largest *trans* influence among these ligands. However, the Ru=*C* chemical shifts of **3** are all larger than that of **1a**, contrary to the higher electron density of the metal ions in the former. We believe that this arises from a competition between the inductive effect and the effect of the porphyrin ring current, whereby the latter is dominant. As shown below, coordination of the ligand L to **1a** would lengthen the Ru=C bond, so that the C atom is less strongly affected by the porphyrin ring current and thus the Ru=*C* chemical shift increases.

In the cases of **1a**-Fe/**1a**, **3a**/**3a**-Os, and **3d**-Fe/**3d**/**3d**-Os, the M=*C* chemical shifts invariably follow the trend Fe > Ru > Os. A parallel trend is also evident for their H_β chemical shifts, except for **1a**-Fe/**1a**, whose H_β chemical shifts are the same within the experimental error. Such trends differ from the Pauling electronegativity trend of Fe < Ru = Os but can be rationalized by competition among the inductive effect, M→por backbonding, and porphyrin ring-current effect. The M→por backbonding, which follows the trend of Fe < Ru < Os for the iron subgroup,[26] increases the electron density of the porphyrin ring and would decrease the H_β chemical shift. If the effect of M→por backbonding outweighs the inductive effect, the expected H_β chemical shift trend should agree with the observed one. On the other hand, a higher electron density in the porphyrin macrocycle would make the C atom of the M=C double bond subject to a larger porphyrin ring current, which would result in a decrease in M=*C* chemical shift. The foregoing observed M=*C* chemical shift trend could indicate that the porphyrin ring-current effect dominates over the inductive effect.

Variation of redox potentials: The redox behavior of metalloporphyrin carbene complexes is an important factor to be considered in inspecting the properties of M=C bonds. From Table 6 it is evident that the first oxidation couples of **1–4** (except **1f**) appear at $E_{1/2}$ = 0.19–0.65 V. This $E_{1/2}$ range covers the $E_{1/2}$ value of 0.42 V for the first oxidation couple of the bis-isocyanide complex **5** but is significantly less anodic than that of [Ru(tpfpp)(CO)] ($E_{1/2}$ = 0.84 V). Since the first oxidation of **5** and [Ru(tpfpp)(CO)] can most reasonably be assigned to metal- and ligand-centered oxidation, respectively, on the basis of electrochemical studies on other bis(isocyanide)ruthenium[18,23] and carbonylruthenium porphyrins,[23] we attribute the first oxidation of **1–4** (except **1f**) to a metal-centered process. This is supported by the spectroelectrochemical studies on **2d**,**h**,**j**,**k** described above. The oxidation couple of **1f**, the second oxidation couples of **2b–d**,**g–i**,**k**, and the third oxidation couple of **2g** have $E_{1/2}$ values comparable to, or more anodic than, that of the first oxidation of [Ru(tpfpp)(CO)]. Such couples can be ascribed to oxidation of the porphyrin ligands. The reduction shown in Table 6 could be due to porphyrin-centered processes.

Since a smaller $E_{1/2}$ value usually corresponds to a higher electron density, comparison of the first-oxidation $E_{1/2}$ values among **1a–c**,**g**; **4a**,**b**; **1a**, **2a–d**,**g–i**; **2j**,**k**; and **3b–d** reveals that the electron density of the ruthenium ion increases with increasing electron-donating capability of the carbene, porphyrin, and *trans* ligands, similar to the above trends for the H_β and/or M=*C* chemical shifts.

Table 6 also reveals that the oxidation of **1a** occurs at a more anodic $E_{1/2}$ value than that of **1a**-Fe. The $E_{1/2}$ value for the first oxidation couple becomes less anodic along the sequence **3d**→**3d**-Fe→**3d**-Os. This trend of $E_{1/2}$ values of Ru > Fe > Os is similar to that obtained by comparing the first oxidation potential among bis-pyridine metalloporphyrins [M(oep)$(py)_2$] with M = Fe, Ru, and Os (−0.15, −0.02, and −0.37 V, respectively).[26b]

Variation of M=C distances: The M=C distance is an important structural feature of a metal–carbene bond, since it can be correlated with the stability/reactivity of metal–carbene complexes. We previously reported a reactive bis(carbene)osmium porphyrin having long Os=C distances of 2.035(2) and 2.027(3) Å and stable monocarbene complex **3a**-Os with a shorter Os=C distance of 1.870(2) Å.[4a] The

significant lengthening of the Fe=C bond in **1a**-Fe upon binding MeIm dramatically enhances its reactivity toward hydrocarbons.[2]

A comparison of the Ru=C bonds among **1a** and **2a**,**i** and between **1a** and **1d** reveals a shorter Ru=C bond for the complex containing a more strongly electron-withdrawing (or less strongly electron-donating) carbene or porphyrin ligand, and thus provides additional examples of the trends derived from comparison of the structures between [Ru(por*){C(Ph)R}] (R = Ph, $CO_2CH_2CH=CH_2$)[3b] and between [Ru(por)(CPh_2)] (por = por*,[3b] tpfpp[16]; see Table 5). The shortening of the Ru=C bond by more strongly electron-withdrawing porphyrin ligands apparently arises from a decrease in the electron density of the ruthenium ion, which increases electron donation from the carbene ligand. However, a more strongly electron-withdrawing carbene group would be less nucleophilic. The shorter Ru=C bonds in the complexes with more strongly electron-withdrawing carbene ligands should have another origin. In fact, the Ru=C bond has two components, Ru←C σ bonding and Ru→C π backbonding, if the carbene groups are considered as neutral "Fischer carbenes". A more strongly electron-withdrawing carbene group would shorten the Ru=C bond by offering stronger Ru→C π backbonding. The overall influence of the electron-withdrawing character of the porphyrin and carbene ligands on the Ru=C distance depends on which of the two bonding components dominates.

Despite previous structure determinations on both five- and six-coordinate ruthenium porphyrin carbene complexes,[3b,10,11a,11b] examination of the *trans* ligand influence on the Ru=CR^1R^2 bond through structural studies on the five- and six-coordinate complexes containing the same [Ru(por)(CR^1R^2)] moiety remained unrealized until recently.[11c] By introducing a strongly electron withdrawing CF_3 group on the diphenylcarbene ligand, Miyamoto et al. obtained complexes [Ru(ttp){C(*m*-$C_6H_4CF_3)_2$}(py)][11b] and [Ru(ttp){C(*m*-$C_6H_4CF_3)_2$}],[11c] both of which were structurally characterized. The Ru=C distance (1.841(6) Å) in the five-coordinate complex [Ru(ttp){C(*m*-$C_6H_4CF_3)_2$}] is 0.027 Å shorter than that in its pyridine adduct [Ru(ttp){C(*m*-$C_6H_4CF_3)_2$}(py)] (1.868(3) Å).[11b]

The present work offers an alternative route to five- and six-coordinate ruthenium porphyrin carbene complexes bearing the same [Ru(por)(CR^1R^2)] moiety. Comparison of the Ru=C distances in **3a**,**b**,**d**,**e** with that in **1a** provides a direct measure of the influence of different *trans* ligands on the Ru=C distance.

The influence of *trans* MeOH, $OPPh_3$, or EtSH ligand on the Ru=C distance is small: coordination of these ligands to **1a** lengthens its Ru=C distance by 0.016 Å or less. A larger *trans* influence was observed for MeIm, whose binding to **1a** increases the Ru=C distance by 0.034 Å (Table 5). However, the *trans* influence of MeIm in the ruthenium porphyrin carbene complex is smaller than in its iron counterpart, as manifested by the 0.06 Å longer Fe=C distance in **3d**-Fe than in **1a**-Fe.[2]

The structure determinations on **3d** and **3d**-Os, together with that on **3d**-Fe,[2] allows a direct comparison to be made among the structures of iron, ruthenium, and osmium porphyrin carbene complexes. Figure 9 shows the side and top views of the structures of the three complexes; their key geometric parameters are compared in Table 8. The $M-N_{por}$ distances average 1.966(3) (Fe), 2.045(2) (Ru), and 2.048(3) Å (Os), slightly shorter than the corresponding average distances of 2.003(2) (Fe), 2.059(7) (Ru), and 2.052(6) Å (Os) in the carbonyl complexes [M(tpp)(CO)(MeIm)] reported by Oldfield et al.[27] The $C_{carbene}$-M-N_{MeIm}

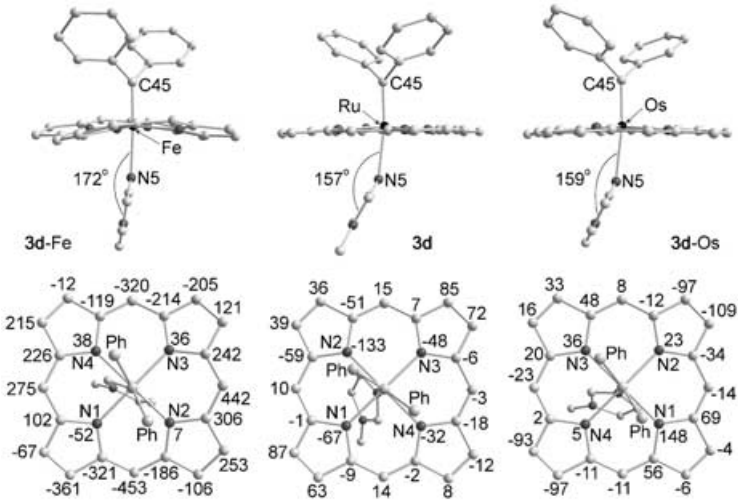

Figure 9. Side- and top-view ball-and-stick representations for the structures of **3d**-Fe,[2] **3d**, and **3d**-Os. For clarity, the hydrogen atoms and the *meso*-C_6F_5 groups are omitted. The deviations [10^{-3} Å] of the porphyrin ring atoms from their least-squares planes are indicated.

Table 8. Comparison of key bond lengths [Å] and angles [°] in **3d**-Fe,[2] **3d**, and **3d**-Os (see Figure 9 for the atom labeling scheme).

	3d-Fe	**3d**	**3d**-Os		**3d**-Fe	**3d**	**3d**-Os
M–N1	1.961(3)	2.053(2)	2.027(3)	M–N2	1.967(3)	2.034(2)	2.061(2)
M–N3	1.964(3)	2.050(2)	2.044(2)	M–N4	1.973(3)	2.043(2)	2.060(2)
C45-M-N5	176.6(2)	172.1(1)	172.7(2)	C45-M-N1	92.8(2)	91.1(1)	93.7(1)
C45-M-N2	91.5(2)	93.7(1)	96.2(1)	C45-M-N3	94.8(2)	96.1(1)	92.0(1)
C45-M-N4	92.4(2)	92.1(1)	92.5(1)	N5-M-N1	83.8(1)	81.2(1)	85.3(1)
N5-M-N2	88.4(2)	84.6(1)	91.1(1)	N5-M-N3	88.7(1)	91.6(1)	89.1(1)
N5-M-N4	87.7(2)	89.7(1)	80.2(1)	N1-M-N2	89.9(2)	89.41(9)	90.3(1)
N1-M-N3	172.4(2)	172.8(1)	174.3(1)	N1-M-N4	89.8(1)	90.17(9)	89.7(1)
N2-M-N3	89.6(2)	90.25(9)	89.3(1)	N2-M-N4	176.1(2)	174.26(9)	171.2(1)
N3-M-N4	90.2(2)	89.46(9)	89.9(1)				

moiety is basically linear in **3d**-Fe (176.6(2)°), but shows a larger distortion from linearity in **3d** (172.1(1)°) and **3d**-Os (172.7(2)°), unlike the rather similar C_{CO}-M-N_{MeIm} angles in [M(tpp)(CO)(MeIm)] (176.7(4)–178.3(3)°; M = Fe, Ru, Os). The observed M=C distances listed in Table 5 (1.827(5), 1.876(3), 1.902(3) Å for **3d**-Fe, **3d**, and **3d**-Os, respectively) follow an order of Fe < Ru < Os, similar to the order of M–CO distances in the carbonyl complexes [M(tpp)(CO)(MeIm)] (1.793(3), 1.83(1), 1.846(9) Å for M = Fe, Ru, Os, respectively).[27]

As depicted in Figure 9, complex **3d**-Fe exhibits a substantially larger porphyrin ring distortion than its ruthenium and osmium counterparts **3d** and **3d**-Os, like the case of [M(tpp)(CO)(MeIm)] with M = Fe, Ru, Os.[27] The carbene planes form appreciably smaller dihedral angles with the closest M–N(por) bonds in the ruthenium and osmium complexes than in the iron counterpart (see Figure 9 and Table 5). The M–N(MeIm) distances in **3d**-Fe (2.168(4) Å), **3d** (2.272(4) Å), and **3d**-Os (2.271(4) Å) (see Table 5) are slightly longer than the respective distances in [M(tpp)(CO)(MeIm)] (M = Fe 2.071(2), Ru 2.185(8), Os 2.175(7) Å).[27] The M–MeIm moieties in **3d** and **3d**-Os are considerably bent, with the imidazole plane and the M–N(MeIm) bond forming a dihedral angle of about 158°. Such a significant bending of the M–MeIm moieties was not observed in [M(tpp)(CO)(MeIm)], whose corresponding dihedral angles for M = Fe, Ru, Os are about 175°.[27]

Conclusion

The present work provides extensive experimental evidence for the influence of carbene substituents, porphyrin substituents, and *trans* ligands on the electronic properties of Ru=C bonds and on the Ru=C distances in ruthenium porphyrin complexes with diaryl and aryl(alkoxycarbonyl) carbene moieties. Electron-withdrawing substituents generally decrease, whereas electron-donating substituents increase, the electron density of the ruthenium ion, and result in shorter and longer Ru=C distances, respectively, regardless of whether these substituents are on the carbene groups or on the porphyrin macrocycles. Weakly coordinating molecules such as methanol exert a small *trans* influence; the *trans* influence of stronger donors such as MeIm is considerably larger, but substantially smaller than that found in the iron counterparts. This provides useful insight into structure–reactivity relationship of ruthenium porphyrin carbene complexes. A direct comparison among iron, ruthenium, and osmium porphyrin carbene complexes reveals a trend in M=C distances of Fe < Ru < Os, and a dramatically smaller porphyrin-ring distortion for ruthenium and osmium. The unique carbene bridge in the solid-state structure of [Ru(tpfpp){C(*p*-$C_6H_4OMe)_2$}] is an unprecedented coordination mode of the carbene group in a metalloporphyrin carbene complex.

Experimental Section

General: All reactions were performed under an argon atmosphere. Pyridine, 1-methylimidazole, triphenylphosphane oxide, diethyl sulfide, *tert*-butyl isocyanide, and ethanethiol were purchased from Aldrich. The solvents (AR grade) were dried according to standard procedures. Diazo compounds N_2CAr_2 (Ar = Ph, *p*-C_6H_4OMe, *p*-C_6H_4Me, *p*-C_6H_4Cl),[28] $N_2C(Ar)CO_2R$ (R = Me, Ar = Ph, *p*-C_6H_4OMe, *p*-$C_6H_4NO_2$; R = Et, Ar = Ph; R = $CH_2CH{=}CH_2$, Ar = Ph),[29] (2*E*,4*E*)-2,4-hexadienyl (*E*)-2-diazo-4-phenyl-3-butenoate,[30] dimethyl diazomalonate,[31] and complexes [Ru(por)(CO)],[32] [Os(tpfpp)(CO)],[4a] [Fe(tpfpp)(CPh_2)] (**1a**-Fe), and [Fe(tpfpp)(CPh_2)(MeIm)] (**3d**-Fe)[2] were prepared by literature methods. UV/Vis spectra (in CH_2Cl_2) were recorded on a HP 8453 Diode Array spectrophotometer, and IR spectra (KBr pellet) on a Bio-Rad FTS165 spectrometer. FAB mass spectra were measured on a Finnigan MAT 95 mass spectrometer; the *m*/*z* value given below for each parent ion or fragment corresponds to the most intense line in the cluster peak (in all cases the observed isotope distribution matches well the theoretically simulated one). ^1H, ^{13}C, and ^{19}F NMR spectra (all in $CDCl_3$) were obtained on a Bruker DPX-300 FT-NMR spectrometer; the chemical shifts are relative to tetramethylsilane (^1H and ^{13}C) or CF_3COOH (^{19}F, $\delta = -76.5$). Cyclic voltammograms were measured on a Bioanalytical Systems (BAS) model 100 B/W electrochemical instrument by employing a conventional two-compartment electrochemical cell (working electrode: glassy carbon, reference electrode: $Ag/AgNO_3$ (0.1 M in CH_3CN), internal reference: $FeCp_2$). Elemental analyses were performed by the Institute of Chemistry, the Chinese Academy of Sciences.

Preparation of [Ru(por)(CR^1R^2)]: A solution of an excess of diazo compound $N_2CR^1R^2$ in dichloromethane (10 mL) was slowly added to a solution of [Ru(por)(CO)] in dichloromethane (5 mL) by syringe pump over 8 h at room temperature. The resulting solution was stirred for 2 h (unless otherwise specified), and then evaporated under reduced pressure. The residue was subjected to chromatography on a silica gel column with dichloromethane/hexane as eluent to give the desired product.

Bis(*p*-chlorophenyl)carbene[5,10,15,20-tetrakis(pentafluorophenyl)porphyrinato]ruthenium, [Ru(tpfpp){C(*p*-$C_6H_4Cl)_2$}] (1b): Reaction conditions: [Ru(tpfpp)(CO)]: 49.6 mg (0.045 mmol), $N_2C(p\text{-}C_6H_4Cl)_2$: 52.6 mg (0.20 mmol), eluent: dichloromethane/hexane 1:1. Yield: 88%; ^1H NMR: $\delta = 8.37$ (s, 8H), 6.11 (d, $J = 8.4$ Hz, 4H), 3.02 (d, $J = 8.3$ Hz, 4H); ^{13}C NMR: $\delta = 322.65$ (Ru=C); UV/Vis: λ_{max} ($\log\varepsilon$) = 386 (4.92), 424 (4.84), 527 (4.10), 552 nm (4.08); elemental analysis (%) calcd for $C_{57}H_{16}Cl_2F_{20}N_4Ru{\cdot}C_6H_{14}$ (1394.88): C 54.25, H 2.17, N 4.02; found: C 54.21, H 1.78, N 4.15; FAB-MS: *m*/*z*: 1309 $[M+H]^+$.

Bis(*p*-tolyl)carbene[5,10,15,20-tetrakis(pentafluorophenyl)porphyrinato]ruthenium, [Ru(tpfpp){C(*p*-$C_6H_4Me)_2$}] (1c): Reaction conditions: [Ru(tpfpp)(CO)]: 49.6 mg (0.045 mmol), $N_2C(p\text{-}C_6H_4Me)_2$: 44.4 mg (0.20 mmol), eluent: dichloromethane/hexane 1:1. Yield: 91%; ^1H NMR: $\delta = 8.29$ (s, 8H), 5.92 (d, $J = 7.7$ Hz, 4H), 3.07 (d, $J = 7.8$ Hz, 4H), 1.76 (s, 6H); ^{13}C NMR: $\delta = 333.00$ (Ru=C); ^{19}F NMR: $\delta = -136.41$ (d), −137.11 (d), −152.59 (t), −162.04 (m); UV/Vis: λ_{max} ($\log\varepsilon$) = 385 (4.85), 426 (4.84), 525 (4.10), 550 nm (4.08); elemental analysis (%) calcd for $C_{59}H_{22}F_{20}N_4Ru$ (1267.87): C 55.89, H 1.75, N 4.42; found: C 56.15, H 1.71, N 4.36; FAB-MS: *m*/*z*: 1268 $[M]^+$.

Bis(*p*-methoxyphenyl)carbene[5,10,15,20-tetrakis(pentafluorophenyl)porphyrinato]ruthenium, [Ru(tpfpp){C(*p*-$C_6H_4OMe)_2$}] (1d): Reaction conditions: [Ru(tpfpp)(CO)]: 49.6 mg (0.045 mmol), $N_2C(p\text{-}C_6H_4OMe)_2$: 50.8 mg (0.20 mmol), eluent: dichloromethane/hexane 2:1. Yield: 90%; ^1H NMR: $\delta = 8.27$ (s, 8H), 6.68 (d, $J = 8.7$ Hz, 4H), 3.41 (s, 6H), 3.15 (d, $J = 8.7$ Hz, 4H); ^{13}C NMR: $\delta = 324.76$ (Ru=C); ^{19}F NMR: $\delta = -136.04$ (d), −136.45 (d), −151.80 (t), −161.20 (m); UV/Vis: λ_{max} ($\log\varepsilon$) = 386 (4.84), 424 (4.75), 526 (4.11), 547 nm (4.09); elemental analysis (%) calcd for $C_{59}H_{22}F_{20}N_4O_2Ru{\cdot}CH_2Cl_2$ (1384.80): C 52.04, H 1.75, N 4.04; found: C 51.97, H 1.69, N 3.95; FAB-MS: *m*/*z*: 1300 $[M]^+$.

Bis(methoxycarbonyl)carbene[5,10,15,20-tetrakis(pentafluorophenyl)porphyrinato]ruthenium, [Ru(tpfpp){C($CO_2Me)_2$}] (1e): Reaction conditions: [Ru(tpfpp)(CO)]: 49.6 mg (0.045 mmol), $N_2C(CO_2Me)_2$: 15.8 mg (0.10 mmol), further stirring time: 24 h, eluent: dichloromethane/hexane 2:1. Yield: 85%; ^1H NMR: $\delta = 8.57$ (s, 8H), 2.20 (s, 6H); ^{13}C NMR: $\delta = 280.49$ (Ru=C); ^{19}F NMR: $\delta = -135.18$ (dd), −136.91 (dd), −151.35 (t), −160.76 (m), −161.36 (m); UV/Vis: λ_{max} ($\log\varepsilon$) = 396 (4.98), 429 (sh,

4.48), 535 (3.97), 565 nm (3.82); elemental analysis (%) calcd for $C_{49}H_{14}F_{20}N_4O_4Ru$ (1203.70): C 48.89, H 1.17, N 4.65; found: C 49.24, H 1.43, N 4.49; FAB-MS: m/z: 1204 $[M]^+$.

***p*-Nitrophenyl(methoxycarbonyl)carbene[5,10,15,20-tetrakis(pentafluorophenyl)porphyrinato]ruthenium, [Ru(tpfpp){C(*p*-$C_6H_4NO_2$)CO_2Me}] (1f)**: Reaction conditions: [Ru(tpfpp)(CO)]: 49.6 mg (0.045 mmol), $N_2C(p\text{-}C_6H_4NO_2)CO_2Me$: 11.9 mg (0.054 mmol), further stirring time: 24 h, eluent: dichloromethane/hexane 2:1. Yield: 90%; ^{1}H NMR: $\delta = 8.51$ (s, 8H), 6.95 (d, $J = 8.6$ Hz, 2H), 3.26 (d, $J = 8.6$ Hz, 2H), 2.24 (s, 3H); ^{13}C NMR: $\delta = 299.44$ (Ru=C); UV/Vis: λ_{max} ($\log\varepsilon$) = 395 (5.06), 426 (sh, 4.62), 533 (4.05), 562 nm (sh, 3.93); elemental analysis (%) calcd for $C_{53}H_{15}F_{20}N_5O_4Ru \cdot 0.5\,C_6H_{14}$ (1309.84): C 51.35, H 1.69, N 5.35; found: C 51.74, H 1.57, N 4.80; FAB-MS: m/z: 1267 $[M]^+$.

***p*-Methoxyphenyl(methoxycarbonyl)carbene[5,10,15,20-tetrakis(pentafluorophenyl)porphyrinato]ruthenium, [Ru(tpfpp){C(*p*-C_6H_4OMe)CO_2Me}] (1g)**: Reaction conditions: [Ru(tpfpp)(CO)]: 49.6 mg (0.045 mmol), $N_2C(p\text{-}C_6H_4OMe)CO_2Me$: 11.1 mg (0.054 mmol), eluent: dichloromethane/hexane 1:1. Yield: 92%; ^{1}H NMR: $\delta = 8.44$ (s, 8H), 5.66 (d, $J = 8.9$ Hz, 2H), 3.39 (d, $J = 8.8$ Hz, 2H), 3.38 (s, 3H), 2.30 (s, 3H); ^{13}C NMR: $\delta = 298.85$ (Ru=C); UV/Vis: λ_{max} ($\log\varepsilon$) = 390 (5.00), 415 (sh, 4.78), 529 (4.19), 550 nm (sh, 4.15); elemental analysis (%) calcd for $C_{54}H_{18}F_{20}N_4O_3Ru \cdot 0.5\,CH_2Cl_2$ (1294.25): C 50.58, H 1.48, N 4.33; found: C 50.21, H 1.64, N 4.35; FAB-MS: m/z: 1252 $[M]^+$.

(*E*)-2-Styryl[(2*E*,4*E*)-2,4-hexadienoxycarbonyl]carbene[5,10,15,20-tetrakis(pentafluorophenyl)porphyrinato]ruthenium, [Ru(tpfpp){C(CH=CHPh)CO_2CH_2(CH=CH)$_2CH_3$}] (1h): Reaction conditions: [Ru(tpfpp)(CO)]: 100.0 mg (0.091 mmol), $N_2C\{(E)\text{-}CH{=}CHPh\}CO_2\text{-}(2E,4E)\text{-}CH_2(CH{=}CH)_2CH_3$: 53.6 mg (0.20 mmol), further stirring time: 24 h, eluent: dichloromethane/hexane 1:1. Yield: 81%; ^{1}H NMR: $\delta = 8.45$ (s, 8H), 7.27 (t, $J = 7.4$ Hz, 1H), 6.86 (t, $J = 7.8$ Hz, 2H), 6.44 (d, $J = 7.8$ Hz, 2H), 5.74–5.44 (m, 3H), 4.94 (d, $J = 16.0$ Hz, 1H), 4.78–4.68 (m, 1H), 3.16 (d, $J = 7.0$ Hz, 2H), 1.84 (d, $J = 15.9$ Hz, 1H), 1.62 (d, $J = 6.8$ Hz, 3H); ^{13}C NMR: $\delta = 288.71$ (Ru=C); ^{19}F NMR: $\delta = -136.22$ (d), -137.67 (s), -152.64 (t), -161.93 (t), -162.35 (s); UV/Vis: λ_{max} ($\log\varepsilon$) = 401 (5.10), 463 (4.17), 530 nm (4.15); elemental analysis (%) calcd for $C_{60}H_{24}F_{20}N_4O_2Ru$ (1313.90): C 54.85, H 1.84, N 4.26; found: C 55.30, H 2.12, N 4.29; FAB-MS: m/z: 1315 $[M+H]^+$.

Diphenylcarbene[5,10,15,20-tetrakis(2,6-dichlorophenyl)porphyrinato]ruthenium, [Ru(tdcpp)(CPh$_2$)] (2a): Reaction conditions: [Ru(tdcpp)(CO)]: 102.0 mg (0.10 mmol), N_2CPh_2: 194 mg (1.0 mmol), further stirring time: 7 d, eluent: dichloromethane/hexane 1:2. Yield: 62%; ^{1}H NMR: $\delta = 8.17$ (s, 8H), 7.75–7.72 (m, 4H), 7.64–7.58 (m, 8H), 6.25 (t, $J = 7.3$ Hz, 2H), 6.06 (t, $J = 7.7$ Hz, 4H), 3.67 (d, $J = 7.7$ Hz, 4H); ^{13}C NMR: $\delta = 327.86$ (Ru=C); UV/Vis: λ_{max} ($\log\varepsilon$) = 390 (4.96), 430 (4.94), 533 (4.15), 560 nm (4.10); elemental analysis (%) calcd for $C_{57}H_{30}Cl_8N_4Ru$ (1155.57): C 59.24, H 2.62, N 4.85; found: C 59.24, H 2.69, N 4.64; FAB-MS: m/z: 1156 $[M]^+$.

Diphenylcarbene[5,10,15,20-tetrakis(4-bromophenyl)porphyrinato]ruthenium, [Ru(4-Br-tpp)(CPh$_2$)] (2b): Reaction conditions: [Ru(4-Br-tpp)(CO)]: 105.8 mg (0.1 mmol), N_2CPh_2: 58.2 mg (0.30 mmol), further stirring time: 24 h, eluent: dichloromethane/hexane 1:2. Yield: 85%; ^{1}H NMR: $\delta = 8.33$ (s, 8H), 7.91 (d, $J = 8.0$ Hz, 4H), 7.85–7.80 (m, 8H), 7.73 (d, $J = 8.2$ Hz, 4H), 6.45 (t, $J = 7.4$ Hz, 2H), 6.13 (t, $J = 7.7$ Hz, 4H), 2.99 (d, $J = 7.1$ Hz, 4H); ^{13}C NMR: $\delta = 319.70$ (Ru=C); UV/Vis: λ_{max} ($\log\varepsilon$) = 396 (5.01), 427 (4.91), 531 nm (4.28); elemental analysis (%) calcd for $C_{57}H_{34}Br_4N_4Ru$ (1195.59): C 57.26, H 2.87, N 4.69; found: C 57.45, H 2.89, N 4.55; FAB-MS: m/z: 1196 $[M]^+$.

Diphenylcarbene[5,10,15,20-tetrakis(4-chlorophenyl)porphyrinato]ruthenium, [Ru(4-Cl-tpp)(CPh$_2$)] (2c): Reaction conditions: [Ru(4-Cl-tpp)(CO)]: 88.0 mg (0.1 mmol), N_2CPh_2: 58.2 mg (0.30 mmol), further stirring time: 24 h, eluent: dichloromethane/hexane 1:2. Yield: 86%; ^{1}H NMR: $\delta = 8.33$ (s, 8H), 7.97 (d, $J = 6.6$ Hz, 4H), 7.79 (d, $J = 6.6$ Hz, 4H), 7.70–7.65 (m, 8H), 6.45 (t, $J = 7.4$ Hz, 2H), 6.14 (t, $J = 7.7$ Hz, 4H), 3.00 (d, $J = 7.3$ Hz, 4H); ^{13}C NMR: $\delta = 319.50$ (Ru=C); UV/Vis: λ_{max} ($\log\varepsilon$) = 396 (5.00), 424 (4.91), 531 nm (4.25); elemental analysis (%) calcd for $C_{57}H_{34}Cl_4N_4Ru$ (1017.79): C 67.26, H 3.37, N 5.50; found: C 67.55, H 3.63, N 5.39; FAB-MS: m/z: 1018 $[M]^+$.

Diphenylcarbene[5,10,15,20-tetrakis(4-fluorophenyl)porphyrinato]ruthenium, [Ru(4-F-tpp)(CPh$_2$)] (2d): Reaction conditions: [Ru(4-F-tpp)(CO)]: 81.4 mg (0.1 mmol), N_2CPh_2: 58.2 mg (0.30 mmol), further stirring time: 24 h, eluent: dichloromethane/hexane 1:2. Yield: 78%; ^{1}H NMR: $\delta = 8.32$ (s, 8H), 8.02–7.98 (m, 4H), 7.86–7.80 (m, 4H), 7.43–7.35 (m, 8H), 6.46 (t, $J = 7.4$ Hz, 2H), 6.15 (t, $J = 7.8$ Hz, 4H), 3.04 (d, $J = 7.9$ Hz, 4H); ^{13}C NMR: $\delta = 318.70$ (Ru=C); UV/Vis: λ_{max} ($\log\varepsilon$) = 395 (5.01), 425 (4.92), 531 nm (4.26); elemental analysis (%) calcd for $C_{57}H_{34}F_4N_4Ru$ (951.97): C 71.92, H 3.60, N 5.89; found: C 72.03, H 3.73, N 5.58; FAB-MS: m/z: 952 $[M]^+$.

Diphenylcarbene(5,10,15,20-tetraphenylporphyrinato)ruthenium, [Ru(tpp)(CPh$_2$)] (2e): Reaction conditions: [Ru(tpp)(CO)]: 74.2 mg (0.1 mmol), N_2CPh_2: 58.2 mg (0.30 mmol), further stirring time: 24 h, eluent: dichloromethane/hexane 1:1. Yield: 89%; ^{1}H NMR: $\delta = 8.34$ (s, 8H), 8.05 (d, $J = 6.7$ Hz, 4H), 7.89 (d, $J = 5.4$ Hz, 4H), 7.70–7.65 (m, 12H), 6.46 (t, $J = 7.4$ Hz, 2H), 6.17 (t, $J = 7.7$ Hz, 4H), 3.04 (d, $J = 7.4$ Hz, 4H); ^{13}C NMR: $\delta = 317.50$ (Ru=C); UV/Vis: λ_{max} ($\log\varepsilon$) = 394 (5.07), 425 (4.96), 530 nm (4.26); elemental analysis (%) calcd for $C_{57}H_{38}N_4Ru$ (880.01): C 77.80, H 4.35, N 6.37; found: C 77.77, H 4.11, N 6.12; FAB-MS: m/z: 880 $[M]^+$.

Diphenylcarbene[5,10,15,20-tetrakis(4-tolyl)porphyrinato]ruthenium, [Ru(ttp)(CPh$_2$)] (2f): Reaction conditions: [Ru(ttp)(CO)]: 79.8 mg (0.1 mmol), N_2CPh_2: 58.2 mg (0.30 mmol), further stirring time: 24 h, eluent: dichloromethane/hexane 1:1. Yield: 86%; ^{1}H NMR: $\delta = 8.36$ (s, 8H), 7.94 (d, $J = 7.6$ Hz, 4H), 7.78 (d, $J = 7.6$ Hz, 4H), 7.53–7.48 (m, 8H), 6.44 (t, $J = 7.4$ Hz, 2H), 6.14 (t, $J = 7.7$ Hz, 4H), 3.02 (d, $J = 7.4$ Hz, 4H), 2.66 (s, 12H); ^{13}C NMR: $\delta = 316.40$ (Ru=C); UV/Vis: λ_{max} ($\log\varepsilon$) = 396 (5.08), 424 (4.94), 532 nm (4.20); elemental analysis (%) calcd for $C_{61}H_{46}N_4Ru$ (936.11): C 78.27, H 4.95, N 5.99; found: C 78.47, H 4.99, N 5.63; FAB-MS: m/z: 936 $[M]^+$.

Diphenylcarbene[5,10,15,20-tetrakis(4-methoxyphenyl)porphyrinato]ruthenium, [Ru(4-MeO-tpp)(CPh$_2$)] (2g): Reaction conditions: [Ru(4-MeO-tpp)(CO)]: 86.2 mg (0.1 mmol), N_2CPh_2: 58.2 mg (0.30 mmol), further stirring time: 24 h, eluent: dichloromethane/hexane 2:1. Yield: 87%; ^{1}H NMR: $\delta = 8.37$ (s, 8H), 7.97 (d, $J = 8.2$ Hz, 4H), 7.80 (d, $J = 8.2$ Hz, 4H), 7.22 (m, 8H), 6.44 (t, $J = 7.4$ Hz, 2H), 6.15 (t, $J = 7.7$ Hz, 4H), 4.07 (s, 12H), 3.01 (d, $J = 7.3$ Hz, 4H); ^{13}C NMR: $\delta = 319.40$ (Ru=C); UV/Vis: λ_{max} ($\log\varepsilon$) = 403 (5.08), 425 (4.93), 534 nm (4.27); elemental analysis (%) calcd for $C_{61}H_{46}N_4O_4Ru$ (1000.11): C 73.26, H 4.64, N 5.60; found: C 73.61, H 4.73, N 5.37; FAB-MS: m/z: 1000 $[M]^+$.

Diphenylcarbene(5,10,15,20-tetramesitylporphyrinato)ruthenium, [Ru(tmp)(CPh$_2$)] (2h): Reaction conditions: [Ru(tmp)(CO)]: 91.0 mg (0.1 mmol), N_2CPh_2: 76.8 mg (0.40 mmol), further stirring time: 10 d, eluent: dichloromethane/hexane 2:1. Yield: 45%; ^{1}H NMR: $\delta = 8.13$ (s, 8H), 7.22 (s, 4H), 7.10 (s, 4H), 6.26 (t, $J = 7.4$ Hz, 2H), 6.03 (t, $J = 7.8$ Hz, 4H), 3.54 (d, $J = 7.2$ Hz, 4H), 2.55 (s, 12H), 1.97 (s, 12H), 1.26 (s, 12H); ^{13}C NMR: $\delta = 318.08$ (Ru=C); UV/Vis: λ_{max} ($\log\varepsilon$) = 395 (5.09), 430 (4.92), 534 (4.03), 562 nm (sh, 3.89); elemental analysis (%) calcd for $C_{69}H_{62}N_4Ru$ (1048.33): C 79.05, H 5.96, N 5.34; found: C 79.40, H 6.32, N 5.41; FAB-MS: m/z: 1049 $[M+H]^+$.

Diphenylcarbene[5,10,15,20-tetrakis(3,4,5-trimethoxyphenyl)porphyrinato]ruthenium, [Ru(3,4,5-MeO-tpp)(CPh$_2$)] (2i): Reaction conditions: [Ru(3,4,5-MeO-tpp)(CO)]: 110.3 mg (0.1 mmol), N_2CPh_2: 58.2 mg (0.30 mmol), further stirring time: 2 d, eluent: diethyl ether/hexane 1:5. Yield: 86%; ^{1}H NMR: $\delta = 8.45$ (s, 8H), 7.32 (s, 4H), 7.13 (s, 4H), 6.43 (t, $J = 7.4$ Hz, 2H), 6.17 (t, $J = 7.7$ Hz, 4H), 4.15 (s, 12H), 4.04 (s, 12H), 3.93 (s, 12H), 3.06 (d, $J = 7.1$ Hz, 4H); ^{13}C NMR: $\delta = 316.30$ (Ru=C); UV/Vis: λ_{max} ($\log\varepsilon$) = 398 (5.06), 424 (4.97), 532 nm (4.24); elemental analysis (%) calcd for $C_{69}H_{62}N_4O_{12}Ru$ (1240.32): C 66.82, H 5.04, N 4.52; found: C 67.01, H 5.10, N 4.43; FAB-MS: m/z: 1241 $[M+H]^+$.

Phenyl(ethoxycarbonyl)carbene[5,10,15,20-tetrakis(2,6-dichlorophenyl)-porphyrinato]ruthenium, [Ru(tdcpp){C(Ph)CO_2Et}] (2j): Reaction conditions: [Ru(tdcpp)(CO)]: 102.0 mg (0.1 mmol), $N_2C(Ph)CO_2Et$: 76.0 mg (0.40 mmol), further stirring time: 2 d, eluent: dichloromethane/hexane 1:1. Yield: 76%; ^{1}H NMR: $\delta = 8.27$ (s, 8H), 7.88–7.75 (m, 4H), 7.65–7.58 (m, 8H), 6.53 (t, $J = 7.4$ Hz, 1H), 6.12 (t, $J = 7.8$ Hz, 2H), 3.82 (d, $J = 7.8$ Hz, 2H), 2.79 (q, $J = 7.2$ Hz, 2H), 0.30 (t, $J = 7.2$ Hz, 3H); ^{13}C NMR: $\delta = 298.50$ (Ru=C); UV/Vis: λ_{max} ($\log\varepsilon$) = 397 (5.03), 427 (sh, 4.72), 538 (4.08), 571 nm (sh, 3.92); elemental analysis (%) calcd for $C_{54}H_{30}Cl_8N_4O_2Ru \cdot 0.5\,CH_2Cl_2$ (1194.00): C 54.82, H 2.62, N 4.69; found: C 54.50, H 2.69, N 4.33; FAB-MS: m/z: 1152 $[M]^+$.

Phenyl(ethoxycarbonyl)carbene(5,10,15,20-tetramesitylporphyrinato)ruthenium, [Ru(tmp){C(Ph)CO_2Et}] (2k): Reaction conditions: [Ru(tmp)-

(CO)]: 91.0 mg (0.1 mmol), $N_2C(Ph)CO_2Et$: 76.0 mg (0.40 mmol), further stirring time: 3 d, eluent: dichloromethane/hexane 1:1. Yield: 70%; ^1H NMR: $\delta = 8.23$ (s, 8H), 7.24 (s, 4H), 7.12 (s, 4H), 6.54 (t, $J = 7.4$ Hz, 1H), 6.07 (t, $J = 7.8$ Hz, 2H), 3.74 (d, $J = 7.3$ Hz, 2H), 2.74 (q, $J = 7.1$ Hz, 2H), 2.56 (s, 12H), 2.12(s, 12H), 1.56 (s, 12H), 0.26 (t, $J = 7.1$ Hz, 3H); ^{13}C NMR: $\delta = 287.50$ (Ru=C); UV/Vis: λ_{max} ($\log\varepsilon$) = 399 (5.12), 434 (sh, 4.64), 538 (4.03), 576 nm (sh, 3.78); elemental analysis (%) calcd for $C_{66}H_{62}N_4O_2Ru$ (1044.29): C 75.91, H 5.98, N 5.37; found: C 75.88, H 6.12, N 5.19; FAB-MS: m/z: 1045 $[M+H]^+$.

Preparation of [Ru(tpfpp)(CPh$_2$)(L)]: These complexes were prepared by recrystallization of [Ru(tpfpp)(CPh$_2$)] from dichloromethane/hexane containing an excess of L (L = MeOH, EtSH, Et_2S, MeIm, py, $OPPh_3$).

Diphenylcarbene[5,10,15,20-tetrakis(pentafluorophenyl)porphyrinato]-methanolruthenium, [Ru(tpfpp)(CPh$_2$)(MeOH)] (3a): Yield: 94%; ^1H NMR: $\delta = 8.24$ (s, 8H), 6.32 (t, $J = 7.5$ Hz, 2H), 6.06 (t, $J = 7.7$ Hz, 4H), 3.08 (d, $J = 7.8$ Hz, 4H); ^{13}C NMR: $\delta = 329.00$ (Ru=C); ^{19}F NMR: $\delta = -135.47$ (d), -136.44 (d), -151.67 (t), -161.16 (m); UV/Vis: λ_{max} ($\log\varepsilon$) = 385 (4.84), 425 (4.83), 525 (4.06), 550 nm (4.04); elemental analysis (%) calcd for $C_{58}H_{22}F_{20}N_4ORu\cdot 0.5\,C_6H_{14}$ (1314.95): C 55.72, H 2.22, N 4.26; found: C 55.70, H 2.12, N 4.23; FAB-MS: m/z: 1240 $[M-MeOH]^+$.

Diphenylcarbene[5,10,15,20-tetrakis(pentafluorophenyl)porphyrinato]-ethanethiolruthenium, [Ru(tpfpp)(CPh$_2$)(EtSH)] (3b): Yield: 96%; ^1H NMR: $\delta = 8.29$ (s, 8H), 6.38 (t, $J = 7.4$ Hz, 2H), 6.13 (t, $J = 7.7$ Hz, 4H), 3.13 (d, $J = 7.6$ Hz, 4H); ^{13}C NMR: $\delta = 330.85$ (Ru=C); UV/Vis: λ_{max} ($\log\varepsilon$) = 385 (4.90), 425 (4.90), 525 (4.12), 550 nm (4.10); elemental analysis (%) calcd for $C_{59}H_{24}F_{20}N_4SRu$ (1301.95): C 54.43, H 1.86, N 4.30; found: C 54.81, H 1.74, N 4.22; FAB-MS: m/z: 1301 $[M-H]^+$.

Diphenylcarbene[5,10,15,20-tetrakis(pentafluorophenyl)porphyrinato]-diethylsulfideruthenium, [Ru(tpfpp)(CPh$_2$)(Et$_2$S)] (3c): Yield: 88%; ^1H NMR: $\delta = 8.26$ (s, 8H), 6.34 (t, $J = 7.4$ Hz, 2H), 6.11 (t, $J = 7.7$ Hz, 4H), 3.11 (d, $J = 8.1$ Hz, 4H), -0.59 (t, $J = 7.4$ Hz, 6H), -0.88 (q, $J = 7.2$ Hz, 4H); ^{13}C NMR: $\delta = 338.34$ (Ru=C); ^{19}F NMR: $\delta = -135.79$ (d), -137.42 (d), -152.71 (t), -161.93 (m), -162.25 (m); UV/Vis: λ_{max} ($\log\varepsilon$) = 385 (4.89), 424 (4.89), 526 (4.12), 549 nm (4.10); elemental analysis (%) calcd for $C_{61}H_{28}F_{20}N_4SRu$ (1330.00): C 55.09, H 2.12, N 4.21; found: C 54.89, H 2.10, N 4.08; FAB-MS: m/z: 1240 $[M-Et_2S]^+$.

Diphenylcarbene[5,10,15,20-tetrakis(pentafluorophenyl)porphyrinato](1-methylimidazole)ruthenium, [Ru(tpfpp)(CPh$_2$)(MeIm)] (3d): Yield: 94%; ^1H NMR: $\delta = 8.13$ (s, 8H), 6.33 (t, $J = 7.4$ Hz, 4H), 6.13 (t, $J = 7.7$ Hz, 4H), 4.95 (br, 1H), 3.21 (d, $J = 7.4$ Hz, 4H), 2.3 (br, 4H), 2.03 (br, 1H); ^{13}C NMR: $\delta = 332.13$ (Ru=C); UV/Vis: λ_{max} ($\log\varepsilon$) = 398 (4.94), 428 (4.88), 528 (4.20), 551 nm (sh, 4.05); elemental analysis (%) calcd for $C_{61}H_{24}F_{20}N_6Ru$ (1321.92): C 55.42, H 1.83, N 6.36; found: C 55.31, H 1.69, N 6.39; FAB-MS: m/z: 1240 $[M-MeIm]^+$.

Diphenylcarbene[5,10,15,20-tetrakis(pentafluorophenyl)porphyrinato]-(triphenylphosphane oxide)ruthenium, [Ru(tpfpp)(CPh$_2$)(OPPh$_3$)] (3e): Yield: 82%; ^1H NMR: $\delta = 8.30$ (s, 8H), 7.53–7.28 (m, 15H), 6.38 (t, $J = 7.4$ Hz, 2H), 6.13 (t, $J = 7.7$ Hz, 4H), 3.14 (d, $J = 7.7$ Hz, 4H); ^{13}C NMR: $\delta = 330.15$ (Ru=C); ^{19}F NMR: $\delta = -136.05$ (d), -137.05 (d), -152.40 (t), -161.88 (m); UV/Vis: λ_{max} ($\log\varepsilon$) = 385 (4.92), 425 (4.92), 526 (4.13), 549 nm (4.12); elemental analysis (%) calcd for $C_{75}H_{33}F_{20}N_4OPRu$ (1518.10): C 59.34, H 2.19, N 3.69; found: C 59.04, H 2.04, N 3.75; FAB-MS: m/z: 1519 $[M+H]^+$.

Diphenylcarbene[5,10,15,20-tetrakis(pentafluorophenyl)porphyrinato]-pyridineruthenium, [Ru(tpfpp)(CPh$_2$)(py)] (3f): Yield: 91%; ^1H NMR: $\delta = 8.18$ (s, 8H), 6.35 (t, $J = 7.4$ Hz, 2H), 6.32 (t, $J = 7.7$ Hz, 1H), 6.14 (t, $J = 7.6$ Hz, 4H), 5.52 (t, $J = 6.5$ Hz, 2H), 3.17 (d, $J = 7.2$ Hz, 4H), 2.62 (br, 2H); ^{13}C NMR: $\delta = 346.69$ (Ru=C); ^{19}F NMR: $\delta = -135.85$ (d), -137.95 (d), -153.01 (t), -162.04 (m), -162.56 (m); UV/Vis: λ_{max} ($\log\varepsilon$) = 390 (4.87), 425 (4.86), 527 (4.01), 550 nm (sh, 3.92); elemental analysis (%) calcd for $C_{62}H_{23}F_{20}N_5Ru$ (1318.92): C 56.46, H 1.76, N 5.31; found: C 56.55, H 1.81, N 5.13; FAB-MS: m/z: 1240 $[M-py]^+$.

Preparation of [Ru(tpfpp){C(Ph)CO$_2$R}(MeOH)]: These complexes were prepared in the same manner as for [Ru(por)(CR^1R^2)] except that the products were recrystallized from dichloromethane/hexane containing methanol.

Phenyl(alloxycarbonyl)carbene[5,10,15,20-tetrakis(pentafluorophenyl)-porphyrinato]methanolruthenium, [Ru(tpfpp){C(Ph)CO$_2$CH$_2$CH=CH$_2$}(MeOH)] (4a): Reaction conditions: [Ru(tpfpp)(CO)]: 49.6 mg (0.045 mmol), $N_2C(Ph)CO_2CH_2CH{=}CH_2$: 9.9 mg (0.049 mmol), eluent: dichloromethane/hexane 1:2. Yield: 94%; ^1H NMR: $\delta = 8.53$ (s, 8H), 6.58 (t, $J = 7.5$ Hz, 1H), 6.16 (t, $J = 7.8$ Hz, 2H), 4.96–4.83 (m, 1H), 4.62 (d, $J = 10.3$ Hz, 1H), 4.37 (d, $J = 17.1$ Hz, 1H), 3.25 (d, $J = 7.2$ Hz, 2H), 3.10 (d, $J = 5.9$ Hz, 2H); ^{13}C NMR: $\delta = 304.34$ (Ru=C); UV/Vis: λ_{max} ($\log\varepsilon$) = 389 (4.99), 422 (sh, 4.77), 530 (4.12), 555 nm (sh, 4.05); elemental analysis (%) calcd for $C_{56}H_{22}F_{20}N_4O_3Ru\cdot MeOH\cdot H_2O$ (1329.89): C 51.48, H 2.12, N 4.21; found: C 51.22, H 1.72, N 4.34; FAB-MS: m/z: 1248 $[M-MeOH]^+$.

Phenyl(methoxycarbonyl)carbene[5,10,15,20-tetrakis(pentafluorophenyl)-porphyrinato]methanolruthenium, [Ru(tpfpp){C(Ph)CO$_2$Me}(MeOH)] (4b): Reaction conditions: [Ru(tpfpp)(CO)]: 49.6 mg (0.045 mmol), $N_2C(Ph)CO_2Me$: 9.5 mg (0.054 mmol), eluent: dichloromethane/hexane 1:2. Yield: 90%; ^1H NMR: $\delta = 8.46$ (s, 8H), 6.54 (t, $J = 7.4$ Hz, 1H), 6.13 (t, $J = 7.7$ Hz, 2H), 3.25 (d, $J = 7.4$ Hz, 2H), 2.26 (s, 3H); ^{13}C NMR: $\delta = 304.13$ (Ru=C); UV/Vis: λ_{max} ($\log\varepsilon$) = 390 (4.97), 420 (sh, 4.78), 530 (4.10), 553 nm (sh, 4.04); elemental analysis (%) calcd for $C_{54}H_{20}F_{20}N_4O_3Ru\cdot 0.5\,C_6H_{14}$ (1296.89): C 52.79, H 2.10, N 4.32; found: C 53.00, H 1.90, N 4.38; FAB-MS: m/z: 1222 $[M-MeOH]^+$.

Phenyl(ethoxycarbonyl)carbene[5,10,15,20-tetrakis(pentafluorophenyl)-porphyrinato]methanolruthenium, [Ru(tpfpp){C(Ph)CO$_2$Et}(MeOH)] (4c): Reaction conditions: [Ru(tpfpp)(CO)]: 49.6 mg (0.045 mmol), $N_2C(Ph)CO_2Et$: 10.3 mg (0.054 mmol), eluent: dichloromethane/hexane 1:2. Yield: 95%; ^1H NMR: $\delta = 8.46$ (s, 8H), 6.56 (t, $J = 7.4$ Hz, 1H), 6.14 (t, $J = 7.8$ Hz, 2H), 3.27 (d, $J = 7.3$ Hz, 2H), 2.66 (q, $J = 7.1$ Hz, 2H), 0.28 (t, $J = 7.1$ Hz, 3H); ^{13}C NMR: $\delta = 305.52$ (Ru=C); UV/Vis: λ_{max} ($\log\varepsilon$) = 388 (4.99), 419 (sh, 4.88), 529 (4.35), 556 nm (sh, 4.32); elemental analysis (%) calcd for $C_{55}H_{22}F_{20}N_4O_3Ru$ (1267.83): C 52.10, H 1.75, N 4.42; found: C 51.71, H 1.83, N 4.18; FAB-MS: m/z: 1236 $[M-MeOH]^+$.

Reaction of [Ru(tpfpp)(CPh$_2$)] (1a) with *tert*-butyl isocyanide: A drop of *tert*-butyl isocyanide was added to a solution of **1a** (24.8 mg, 0.02 mmol) in dichloromethane (5 mL). The solution was immediately evaporated to dryness. The residue was purified by chromatography on a silica gel column with dichloromethane/hexane 1:2 as eluent.

[5,10,15,20-Tetrakis(pentafluorophenyl)porphyrinato]bis(*tert*-butylisocyanide)ruthenium, [Ru(tpfpp)(C≡N*t*Bu)$_2$] (5): Yield: 85%; ^1H NMR: $\delta = 8.36$ (s, 8H), -0.46 (s, 18H); ^{13}C NMR: $\delta = 182.14$ (C≡N); UV/Vis: λ_{max} ($\log\varepsilon$) = 395 (4.80), 415 (5.59), 512 nm (4.16); IR: $\tilde{\nu} = 2133$, 2007 cm^{-1} (C≡N); elemental analysis (%) calcd for $C_{54}H_{26}F_{20}N_6Ru$ (1239.86): C 52.31, H 2.11, N 6.78; found: C 52.33, H 2.04, N 7.16; FAB-MS: m/z: 1241 $[M+H]^+$.

Preparation of [Os(tpfpp)(CPh$_2$)(MeIm)]: This complex was prepared in the same manner as [Ru(tpfpp)(CPh$_2$)][16] except that [Os(tpfpp)(CO)] was used instead of [Ru(tpfpp)(CO)] and the product was recrystallized from dichloromethane/hexane containing 1-methylimidazole. Reaction conditions: [Os(tpfpp)(CO)]: 97.6 mg (0.082 mmol), N_2CPh_2: 15.9 mg (0.082 mmol), eluent: dichloromethane/hexane 2:1.

Diphenylcarbene[5,10,15,20-tetrakis(pentafluorophenyl)porphyrinato](1-methylimidazole)osmium, [Os(tpfpp)(CPh$_2$)(MeIm)] (3d-Os): Yield: 70%; ^1H NMR: $\delta = 7.44$ (s, 8H), 6.44 (t, $J = 7.4$ Hz, 2H), 6.17 (t, $J = 7.6$ Hz, 4H), 5.20 (s, 1H), 4.14 (d, $J = 7.3$ Hz, 4H), 2.78 (s, 1H), 2.51 (s, 1H), 2.47 (s, 3H); ^{13}C NMR: $\delta = 289.27$ (Os=C); UV/Vis: λ_{max} ($\log\varepsilon$) = 385 (4.65, sh), 408 (4.86), 519 (4.13), 546 nm (4.12); elemental analysis (%) calcd for $C_{61}H_{24}F_{20}N_6Os$ (1412.13): C 51.92, H 1.71, N 5.96; found: C 51.53, H 1.50, N 6.15; FAB-MS: m/z: 1412 $[M]^+$.

X-ray crystal structure determinations of 1d, 2a,i, 3a,b,d,e, 4a–c, and 3d-Os: Diffraction-quality crystals were obtained by slow evaporation of solutions in dichloromethane/hexane (**1d**, **2a**,**i**), dichloromethane/methanol (**3a**, **4a–c**), dichloromethane/ethanethiol (**3b**), and dichloromethane/hexane containing 1-methylimidazole (**3d**, **3d**–Os) or triphenylphosphane oxide (**3e**) at room temperature. The data were collected on a MAR diffractometer with a 300 mm image plate detector or on a Bruker CCD SMART system using graphite-monochromatized $Mo_{K\alpha}$ radiation ($\lambda = 0.71073$ Å). The structures were refined by full-matrix least-squares procedures on F^2 by employing the SHELXL programs. There are two independent molecules (a and b) in the unit cell of **3a**·MeOH, which are linked together by hydrogen bonds (see Figure 5). The carbon atom in one of the 12 methoxyl groups of the 3,4,5-MeO-tpp macrocycle in the structure of **2i** (C55), and the carbon atoms in the ethanethiol axial ligand in the structure of **3b** (C58 and C59) are disordered.

CCDC-224978 (**1d**·CH_2Cl_2), -224979 (**2a**·CH_2Cl_2), -224980 (**2i**·CH_2Cl_2), -224981 (**3a**·MeOH), -224982 (**3b**), -224983 (**3d**), -224985 (**3e**), -224986 (**4a**·MeOH), -224987 (**4b**), -224988 (**4c**·MeOH) and -224984 (**3d**-Os) contain the supplementary crystallographic data for this paper. These data can be obtained free of charge via www.ccdc.cam.ac.uk/conts/retrieving.html (or from the Cambridge Crystallographic Data Centre, 12 Union Road, Cambridge CB2 1EZ, UK; fax: (+44) 1223-336-033; or deposit@ccdc.cam.uk).

Acknowledgments

This work was supported by the Generic Drug Research Program of The University of Hong Kong, the Hong Kong University Foundation, the Hong Kong Research Grants Council, and the University Grants Committee of the Hong Kong SAR of China (Area of Excellence Scheme, AoE/P-10/01). C.M.C. is grateful for a NSFC Young Researcher Award administrated by the NSF of China.

[1] Selected reviews on transition metal carbene complexes: a) D. J. Cardin, B. Cetinkaya, M. F. Lappert, *Chem. Rev.* **1972**, *72*, 545; b) M. Brookhart, W. B. Studabaker, *Chem. Rev.* **1987**, *87*, 411; c) M. P. Doyle in *Comprehensive Organometallic Chemistry II, Vol. 12* (Ed.: L. S. Hegedus), Pergamon, Oxford, **1995**, Chapter 5.1, p. 387, and Chapter 5.2, p. 421; d) L. S. Hegedus, *Acc. Chem. Res.* **1995**, *28*, 299; e) C. Pariya, K. N. Jayaprakash, A. Sarkar, *Coord. Chem. Rev.* **1998**, *168*, 1; f) M. P. Doyle, D. C. Forbes, *Chem. Rev.* **1998**, *98*, 911; g) J. W. Herndon, *Coord. Chem. Rev.* **2000**, *206*, 237; h) M. R. Buchmeiser, *Chem. Rev.* **2000**, *100*, 1565; i) T. M. Trnka, R. H. Grubbs, *Acc. Chem. Res.* **2001**, *34*, 18; j) C.-M. Che, J.-S. Huang, *Coord. Chem. Rev.* **2002**, *231*, 151.

[2] Y. Li, J.-S. Huang, Z.-Y. Zhou, C.-M. Che, X.-Z. You, *J. Am. Chem. Soc.* **2002**, *124*, 13185.

[3] a) W.-C. Lo, C.-M. Che, K.-F. Cheng, T. C. W. Mak, *Chem. Commun.* **1997**, 1205; b) C.-M. Che, J.-S. Huang, F.-W. Lee, Y. Li, T.-S. Lai, H.-L. Kwong, P.-F. Teng, W.-S. Lee, W.-C. Lo, S.-M. Peng, Z.-Y. Zhou, *J. Am. Chem. Soc.* **2001**, *123*, 4119; c) J.-L. Zhang, H.-B. Zhou, J.-S. Huang, C.-M. Che, *Chem. Eur. J.* **2002**, *8*, 1554.

[4] a) Y. Li, J.-S. Huang, Z.-Y. Zhou, C.-M. Che, *J. Am. Chem. Soc.* **2001**, *123*, 4843; b) Y. Li, J.-S. Huang, Z.-Y. Zhou, C.-M. Che, *Chem. Commun.* **2003**, 1362.

[5] a) D. A. Smith, D. N. Reynolds, L. K. Woo, *J. Am. Chem. Soc.* **1993**, *115*, 2511; b) J. R. Wolf, C. G. Hamaker, J.-P. Djukic, T. Kodadek, L. K. Woo, *J. Am. Chem. Soc.* **1995**, *117*, 9194; c) C. G. Hamaker, G. A. Mirafzal, L. K. Woo, *Organometallics* **2001**, *20*, 5171; d) C. G. Hamaker, J.-P. Djukic, D. A. Smith, L. K. Woo, *Organometallics* **2001**, *20*, 5189.

[6] a) E. Galardon, P. Le Maux, G. Simonneaux, *Chem. Commun.* **1997**, 927; b) E. Galardon, S. Roué, P. Le Maux, G. Simonneaux, *Tetrahedron Lett.* **1998**, *39*, 2333; c) E. Galardon, P. Le Maux, G. Simonneaux, *Tetrahedron* **2000**, *56*, 615; d) C. Paul-Roth, F. De Montigny, G. Rehtore, G. Simonneaux, M. Gulea, S. Masson, *J. Mol. Catal. A* **2003**, *201*, 79.

[7] M. Frauenkron, A. Berkessel, *Tetrahedron Lett.* **1997**, *38*, 7175.

[8] Z. Gross, N. Galili, L. Simkhovich, *Tetrahedron Lett.* **1999**, *40*, 1571.

[9] a) J. P. Collman, P. J. Brothers, L. McElwee-White, E. Rose, L. J. Wright, *J. Am. Chem. Soc.* **1985**, *107*, 4570; b) J. P. Collman, P. J. Brothers, L. McElwee-White, E. Rose, *J. Am. Chem. Soc.* **1985**, *107*, 6110; c) J. P. Collman, E. Rose, G. D. Venburg, *J. Chem. Soc. Chem. Commun.* **1993**, 934.

[10] E. Galardon, P. Le Maux, L. Toupet, G. Simonneaux, *Organometallics* **1998**, *17*, 565.

[11] a) M. Kawai, H. Yuge, T. K. Miyamoto, *Acta Crystallogr. Sect. C* **2002**, *58*, M581; b) T. Harada, S. Wada, H. Yuge, T. K. Miyamoto, *Acta Crystallogr. Sect. C* **2003**, *59*, M37; c) S. Wada, H. Yuge, T. K. Miyamoto, *Acta Crystallogr. Sect. C* **2003**, *59*, M369.

[12] For previously reported osmium porphyrin carbene complexes, see: refs. [4, 5a, d]; b) L. K. Woo, D. A. Smith, *Organometallics* **1992**, *11*, 2344; c) J.-P. Djukic, D. A. Smith, V. G. Young, Jr., L. K. Woo, *Organometallics* **1994**, *13*, 3020; d) J.-P. Djukic, V. G. Young, Jr., L. K. Woo, *Organometallics* **1994**, *13*, 3995.

[13] For previously reported iron porphyrin carbene complexes, see: ref. [2]; b) D. Mansuy, M. Lange, J.-C. Chottard, P. Guerin, P. Morliere, D. Brault, M. Rougee, *J. Chem. Soc. Chem. Commun.* **1977**, 648; c) D. Mansuy, M. Lange, J.-C. Chottard, J. F. Bartoli, B. Chevrier, R. Weiss, *Angew. Chem.* **1978**, *90*, 828; *Angew. Chem. Int. Ed. Engl.* **1978**, *17*, 781; d) D. Mansuy, *Pure Appl. Chem.* **1980**, *52*, 681; e) D. Mansuy, *Pure Appl. Chem.* **1987**, *59*, 759; f) I. Artaud, N. Gregoire, J.-P. Battioni, D. Dupre, D. Mansuy, *J. Am. Chem. Soc.* **1988**, *110*, 8714; g) I. Artaud, N. Gregoire, P. Leduc, D. Mansuy, *J. Am. Chem. Soc.* **1990**, *112*, 8714.

[14] Electrochemical studies on metalloporphyrin carbene complexes are extremely rare. The only report on such studies appeared about 20 years ago and deals with iron porphyrin heteroatom-stabilized carbene and vinylcarbene complexes: J.-P. Battioni, D. Lexa, D. Mansuy, J.-M. Savéant, *J. Am. Chem.* Soc. **1983**, *105*, 207.

[15] Abbreviations for the porphyrinato dianions: $(tpfpp)^{2-}$ = 5,10,15,20-tetrakis(pentafluorophenyl)porphyrinato, $(tdcpp)^{2-}$ = 5,10,15,20-tetrakis(2,6-dichlorophenyl)porphyrinato, $(4\text{-Br-tpp})^{2-}$ = 5,10,15,20-tetrakis(4-bromophenyl)porphyrinato, $(4\text{-Cl-tpp})^{2-}$ = 5,10,15,20-tetrakis(4-chlorophenyl)porphyrinato, $(4\text{-F-tpp})^{2-}$ = 5,10,15,20-tetrakis(4-fluorophenyl)porphyrinato, $(tpp)^{2-}$ = 5,10,15,20-tetraphenylporphyrinato, $(ttp)^{2-}$ = 5,10,15,20-tetrakis(4-tolyl)porphyrinato, $(4\text{-MeO-tpp})^{2-}$ = 5,10,15,20-tetrakis(4-methoxyphenyl)porphyrinato, $(tmp)^{2-}$ = 5,10,15,20-tetramesitylporphyrinato, $(3,4,5\text{-MeO-tpp})^{2-}$ = 5,10,15,20-tetrakis(3,4,5-trimethoxyphenyl)porphyrinato. For simplicity, the 2− charge on these ligands are not shown in the text and in Table 6.

[16] Y. Li, P. W. H. Chan, N. Zhu, C.-M. Che, *Organometallics* **2004**, *23*, 54.

[17] tmtaa = dibenzotetramethyltetraaza[14]annulene dianion; b) A. Klose, E. Solari, J. Hesschenbrouck, C. Floriani, N. Re, S. Geremia, L. Randaccio, *Organometallics* **1999**, *18*, 360.

[18] F.-W. Lee, M.-Y. Choi, K.-K. Cheung, C.-M. Che, *J. Organomet. Chem.* **2000**, *595*, 114.

[19] a) J. P. Collman, T. N. Sorrell, K. O. Hodgson, A. K. Kulshrestha, C. E. Strouse, *J. Am. Chem. Soc.* **1977**, *99*, 5180; b) S. W. McCann, F. V. Wells, H. H. Wickman, T. N. Sorrell, J. P. Collman, *Inorg. Chem.* **1980**, *19*, 621.

[20] a) B. R. James, A. Pacheco, S. J. Rettig, J. A. Ibers, *Inorg. Chem.* **1988**, *27*, 2414; b) A. Pacheco, B. R. James, S. J. Rettig, *Inorg. Chem.* **1995**, *34*, 3477; $(oep)^{2-}$ = 2,3,7,8,12,13,17,18-octaethylporphyrinato dianion.

[21] Note that **1d** is readily soluble in dichloromethane and chloroform, and its ^1H NMR spectrum in $CDCl_3$ shows no signals that are assignable to an axial *trans* ligand. Therefore, in solution, this complex should be a five-coordinate monomer.

[22] For examples, see a) J. T. Landrum, C. A. Reed, K. Hatano, W. R. Scheidt, *J. Am. Chem. Soc.* **1978**, *100*, 3232; b) J. T. Landrum, K. Hatano, W. R. Scheidt, C. A. Reed, *J. Am. Chem. Soc.* **1980**, *102*, 6729; c) M. J. Gunter, G. M. McLaughlin, K. J. Berry, K. S. Murray, M. Irving, P. E. Clark, *Inorg. Chem.* **1984**, *23*, 283; d) J. P. Collman, J. T. McDevitt, C. R. Leidner, G. T. Yee, J. B. Torrance, W. A. Little, *J. Am. Chem. Soc.* **1987**, *109*, 4606; e) K. Liou, M. Y. Ogawa, T. P. Newcomb, G. Quirion, M. Lee, M. Poirier, W. P. Halperin, B. M. Hoffman, J. A. Ibers, *Inorg. Chem.* **1989**, *28*, 3889; f) E. B. Fleischer, A. M. Shachter, *Inorg. Chem.* **1991**, *30*, 3763; g) P. Turner, M. J. Gunter, T. W. Hambley, A. H. White, B. W. Skelton, *Inorg. Chem.* **1992**, *31*, 2295; h) R. K. Kumar, S. Balasubramanian, I. Goldberg, *Chem. Commun.* **1998**, 1435; i) E. J. Brandon, R. D. Rogers, B. M. Burkhart, J. S. Miller, *Chem. Eur. J.* **1998**, *4*, 1938; j) Y. Diskin-Posner, G. K. Patra, I. Goldberg, *J. Chem. Soc. Dalton Trans.* **2001**, 2775.

[23] For a review on electrochemical studies on metalloporphyrins, see a) K. M. Kadish, *Prog. Inorg. Chem.* **1986**, *34*, 435; b) J. W. Buchler, C. Dreher, F. M. Kunzel, *Struct. Bonding (Berlin)* **1995**, *84*, 1; c) K. M. Kadish, E. van Camelbecke, G. Royal in *Porphyrin Handbook, Vol. 8* (Eds.: K. M. Kadish, K. M. Smith, R. Guilard), Academic Press, San Diego, **2000**, pp. 1–114.

[24] a) G. M. Brown, F. R. Hopf, J. A. Ferguson, T. J. Meyer, D. G. Whitten, *J. Am. Chem. Soc.* **1973**, *95*, 5939; b) D. Dolphin, B. R. James,

A. J. Murray, J. R. Thornback, *Can. J. Chem.* **1980**, *58*, 1125; c) T. Malinski, D. Chang, L. A. Bottomley, K. M. Kadish, *Inorg. Chem.* **1982**, *21*, 4248.
[25] a) H. Scheer, J. J. Katz in *Porphyrins and Metalloporphyrins* (Ed.: K. M. Smith), Elsevier, Amsterdam, **1975**, Chapter 10, pp. 460–462; b) A. Antipas, J. W. Buchler, M. Gouterman, P. D. Smith, *J. Am. Chem. Soc.* **1980**, *102*, 198.
[26] a) G. M. Brown, F. R. Hopf, T. J. Meyer, D. G. Whitten, *J. Am. Chem. Soc.* **1975**, *97*, 5385; b) J. W. Buchler, W. Kokisch, P. D. Smith in *Struct. Bonding (Berlin)*, *Vol. 34* (Ed.: J. D. Dunitz), Springer, New York, **1978**, p. 79.
[27] R. Salzmann, C. J. Ziegler, N. Godbout, M. T. McMahon, K. S. Suslick, E. Oldfield, *J. Am. Chem. Soc.* **1998**, *120*, 11323.
[28] J. B. Miller, *J. Org. Chem.* **1959**, *24*, 560.
[29] Z. Qu, W. Shi, J. Wang, *J. Org. Chem.* **2001**, *66*, 8139.
[30] H. M. L. Davies, B. D. Doan, *J. Org. Chem.* **1999**, *64*, 8501.
[31] M. Regitz, J. Hocker, A. Liedhegener, *Org. Syn. Coll. Vol. V* **1973**, 179.
[32] a) J. S. Lindsey, R. W. Wagner, *J. Org. Chem.* **1989**, *54*, 828; b) M. Tsutsui, D. Ostfeld, L. M. Hoffman, *J. Am. Chem. Soc.* **1971**, *93*, 1820; c) D. P. Rillema, J. K. Nagle, L. F. Barringer, Jr., T. J. Meyer, *J. Am. Chem. Soc.* **1981**, *103*, 56. Note that the formulation [Ru(por)(CO)] is just used for simplicity, since such complexes may contain oxygen-donor solvents or water in the axial sites (see ref. [23b]).

Received: November 28, 2003
Revised: March 9, 2004
Published online: May 26, 2004

